Plant Stress 18 (2025) 101009

Contents lists available at ScienceDirect

Plant Stress

journal homepage: www.sciencedirect.com/journal/plant-stress

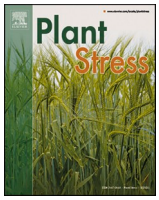

Dynamics of the Spanish fir transcriptome in nature: Metabolic pathways and gene networks involved in the response to climate stress

Irene Blanca-Reyes [a,1], María Torés-España [a,1], Victor Lechuga [b], María Teresa Llebrés [a], Fernando N. de la Torre [a], José A. Carreira [b], Concepción Avila [a], Francisco M. Cánovas [a,*], Vanessa Castro-Rodríguez [a,*]

[a] Grupo de Biología Molecular y Biotecnología, Departamento de Biología Molecular y Bioquímica, Universidad de Málaga, Campus Universitario de Teatinos, 29071 Málaga, Spain
[b] Center for Advanced Studies on Earth Sciences, Energy and Environment (CEACTEMA), Universidad de Jaén, Campus Las Lagunillas s/n., 23009 Jaén, Spain

ARTICLE INFO

Keywords:
Conifers
Mediterranean forests
Abies pinsapo
Transcriptome
Climate change
Aromatic amino acids
Phenolics

ABSTRACT

Circum-Mediterranean firs, and particularly the relic Spanish-fir from the south of the Iberian Peninsula (*Abies pinsapo* Boiss.), are among the most drought-sensitive and vulnerable to climate change within the broad context of Mediterranean forest species. Forest decline and die-back episodes associated to warming trends and recurrent droughts of increasing duration and intensity in the last decades point to an increasing vulnerability of *A. pinsapo* local populations. In this work, physiological and transcriptional analyses were combined to assess the response of trees growing in natural forests under contrasting conditions. The results show a modulation of the transcriptome in response to climatic stress with substantial changes in the expression of genes involved in water stress, aromatic amino acid metabolism, and transcription factors associated with the transcriptional regulation of the observed patterns of gene expression. Roots were determined to be the primary organs involved in the transcriptional response to stress, which may be mediated by a gene-network including interactions among structural and regulatory genes. Interactive elements comprise genes encoding stress-related proteins of the ApLEA family, ApADH, the first committed enzyme in tyrosine biosynthesis, and root-specific transcription factors implicated in stress regulation belonging to the ApERF, ApYABBY, and ApNAC superfamilies. Data provide new insights to understand the response of Spanish firs to current climatic pressure by the identification of individual genes and gene-networks potentially involved in local adaptation. This new knowledge will facilitate comparative studies of gene variation in the Spanish fir populations using the identified genes as molecular markers for the selection of the best adapted genotypes in the response to climate stress.

1. Introduction

Forests are essential ecosystem service providers regarding global carbon fixation and the maintenance of biodiversity worldwide (Brockerhoff et al., 2017; Felipe-Lucia et al., 2018). They also provide a wide range of products with significant economic value for society, including wood, fiber, resins, renewable energy and various metabolites valuable for pharmaceutical and industrial applications. However, this provision of services is increasingly threatened by the accelerating impacts, both direct and indirect, of global warming on forests (Mina et al., 2017). Spatially extensive mortality events and forest decline processes have been documented worldwide over the last few decades (Allen et al., 2010; Hartmann et al., 2022). This suggests a limited phenotypic plasticity or adaptive potential to cope with ongoing climatic trends (Anderegg et al., 2019).

Climate change risks to forest health are of particular importance in the Mediterranean basin, especially in the Iberian Peninsula which is one of the most vulnerable areas of Europe to increasing aridity (Gazol et al., 2018; DeSoto et al., 2020). Therefore, it is urgent the adoption of measures aimed at fostering the resilience of these forest ecosystems,

* Corresponding authors.
E-mail addresses: ireneblanca@uma.es (I. Blanca-Reyes), m.tor.es2399@gmail.com (M. Torés-España), vlechuga@ujaen.es (V. Lechuga), m.llebres@uma.es (M.T. Llebrés), fdelatorre@uma.es (F.N. de la Torre), jafuente@ujaen.es (J.A. Carreira), cavila@uma.es (C. Avila), canovas@uma.es (F.M. Cánovas), vavicaro@uma.es (V. Castro-Rodríguez).
[1] These authors contributed equally to work.

https://doi.org/10.1016/j.stress.2025.101009
Received 28 February 2025; Received in revised form 15 August 2025; Accepted 25 August 2025
Available online 26 August 2025

prioritizing actions on those with high ecological and conservation value. In the context of Mediterranean forests, modelling forecasts based on tree-growth sensitivity to climate extremes and warming trends point to critical vulnerability in a near future for many of the circum-Mediterranean fir species and, particularly, for the Spanish fir *A. pinsapo* (Sánchez-Salguero et al., 2017). In fact, *A. pinsapo* forests showed the earliest symptoms of climate-change induced forest dieback and mortality in the Iberian peninsula (Linares et al., 2009).

The Spanish fir (*Abies pinsapo* Boiss.), a member of the Pinaceae family endemic from north-facing, 1000–1800 m asl, slopes in coastal mountains at the southern Iberian Peninsula, is a climatic relict species that survived Holocene ice-age cycles in small glacial refugia (Linares 2011). Currently subjected to the constraints of Mediterranean-type climate seasonality (long, hot and dry summers), further studies have shown impaired water and carbon use in the trees since the early 1990s in response to rising temperatures and prolonged droughts (Sánchez-Salguero et al., 2015; Lechuga et al., 2019) as well as increasing sensitivity to biotic and abiotic stresses (Navarro-Cerrillo et al., 2022). Finally, intra-specific competition have been shown to be a strong modulator of *A. pinsapo* ecophysiological and tree-growth responses to climatic stress, both in natural and thinned forest stands (Linares et al., 2010; Lechuga et al., 2017). This scenario has recently worsened due to unprecedent periods of drought and persistent warming during the dry seasons in recent years (2022–2024).

Local variations in resilience associated to contrasting stand structure and microclimatic conditions have been assessed by niche distribution and habitat suitability modelling across *A. pinsapo* populations, being those located at the lower ecotone the most vulnerable (Blanco-Cano et al., 2022). Understanding the molecular basis behind the differential adaptability of local populations to climatic stresses is of major relevance, both from fundamental and applied perspectives. Blanca-Reyes et al. (2024) found that trees from these more vulnerable populations were expressing higher levels of stress-related genes. It is known that adaptive traits in forest trees to abiotic stresses are controlled by numerous genes (Aitken et al., 2008; De la Torre et al., 2022). Thus, identifying individual genes and their variation within natural populations is a crucial step toward understanding the molecular basis of forest trees' adaptive capacities. Additionally, these genes can be used as molecular tools for selecting populations better adapted to current and predicted climatic disturbances.

The vast size and the highly repetitive nature of conifer genomes (15–25 Gb) have limited structural and functional genomics in this major group of seed plants (De La Torre et al., 2014; Cañas et al., 2019). However, advances in next generation sequencing (NGS) platforms, including the recent implementation of those based on single-molecule sequencing, have led to significant progress in understanding the genetic and cellular processes underlying tree growth and survival (Street, 2019; Allona et al., 2019). Functional genomic resources and molecular markers for *A. pinsapo* are now available (Pérez-González et al., 2018; Ortigosa et al., 2022; Cobo-Simón et al., 2023; Blanca-Reyes et al., 2024), and the sequencing and assembly of the genome is underway (Castro-Rodríguez, 2024). Genomic approaches are now suitable for the identification of local populations of Spanish fir exhibiting better adaptation to the threats of climatic crisis. The molecular and functional characterization of individual genes involved in the response to environmental stresses is a necessary step for developing adaptation strategies to mitigate the effects of climate change. Identifying gene networks functionally related to climate stress will facilitate the development of conservation strategies-based on the selection of better adapted trees using genomic tools and assisted migration programs based on the use of seedlings exhibiting high genetic variability.

In the present work, the physiological and molecular responses of Spanish fir (*A. pinsapo*) to climate-driven stresses were investigated in trees growing under natural conditions. The physiological status of the trees was assessed, and transcriptomic changes in the needles and roots were compared in two local populations differing in their geographical distribution and climatic features. The results indicate that trees with lower physiological performance, located at a lower ecotone, exhibited a major impact of climatic factors on the transcriptomes of their needles and roots, than trees located at higher altitude. Functional enrichment analysis of differentially expressed genes in both populations identified metabolic pathways and transcription factors potentially involved in the adaptation to climatic stress.

2. Material and methods

2.1. Plant material and experimental design

Plant material was harvested in the "Sierra de las Nieves" National Park, located in the province of Málaga (south of Spain), which hosts the largest population of Spanish fir forests. To examine the effect of between-sites, and within-site intra-annual, climatic variations on the tree transcriptome dynamics, tissue samples from two different organs (needles and roots) were collected at two sites and two seasons. Sample collection was accomplished at two geographically close but microclimatically distinct locations (Fig. 1): Puerto Saucillo-Yunquera (lower ecotone, 1100–1200 m asl; hereafter referred to as YUN) and Cañada del Cuerno-Ronda (upper ecotone, 1700–1800 m asl; hereafter referred to as RON) (Fig. 1a). At each site, field sampling was conducted twice during the same hydrological year (hydrological years for Mediterranean-type ecosystems comprise from September of year i to August of year $i+1$): in September 2022 (autumn onset, end of hot and dry season, water limitation peak; hereafter referred to as AUT) and in May 2023 (mid spring, warm and wet season, vegetative growth peak; hereafter referred *As spr*). These two time points were selected to represent the most contrasting intra-annual climatic conditions affecting tree performance at the study sites. For each site and time point, $n = 3$ biological replicates were collected for transcriptome analysis to account for environmental variability inherent to natural field conditions (Fig. 1b). Samples were harvested from individual trees carefully selected after extensive gene expression analyses performed in 10 trees from each location (Blanca-Reyes et al., 2024). This accomplishment ensures they represent a scenario of variation in each population, thus providing a robust basis for the transcriptomic analysis.

On each occasion, needles and roots were harvested at midday from ten randomly selected adult individuals (30–50 yr-old trees) of *A. pinsapo*. Samples were immediately frozen in liquid N and disposed of in dry ice for transporting to the laboratory where they were stored at −80 °C. Subsequently, frozen samples were independently homogenized using a Mixer Mills MM400 (Retsch) and further stored at −80 °C until use. Total intact RNA was extracted from independent samples, purified and processed for library construction, sequencing and bioinformatic analyses of RNA-seq data (Fig. 1c).

At the same time as the collection of tissue samples for gene expression analyses, gas exchange measurements (net photosynthesis and stomatal conductance to water) were carried out in the same trees by using a portable infrared gas analyser (IRGA) LI-6400 coupled to a LI-6400–05 conifer chamber, all from LI-COR Inc. (Lincoln, Nebraska, USA). In all the cases, before the measuring set, the device was calibrated in situ. In each site, sampling date and tree, measurements were made on a twig terminus carrying 1- to 3-year-old needles, in the central hours of the day. Measurements were averaged for each tree. Each measurement lasted 90 s, taking one data measurement every 5 s (18 repeated measurements per sampling event), and the measurements began when net photosynthesis and stomatal conductance rates were steady.

2.2. RNA isolation and reverse-transcription quantitative PCR (RT-qPCR)

Total RNA extraction was carried out following the method described by Canales et al. (2012). Briefly, 100 mg of *A. pinsapo* samples

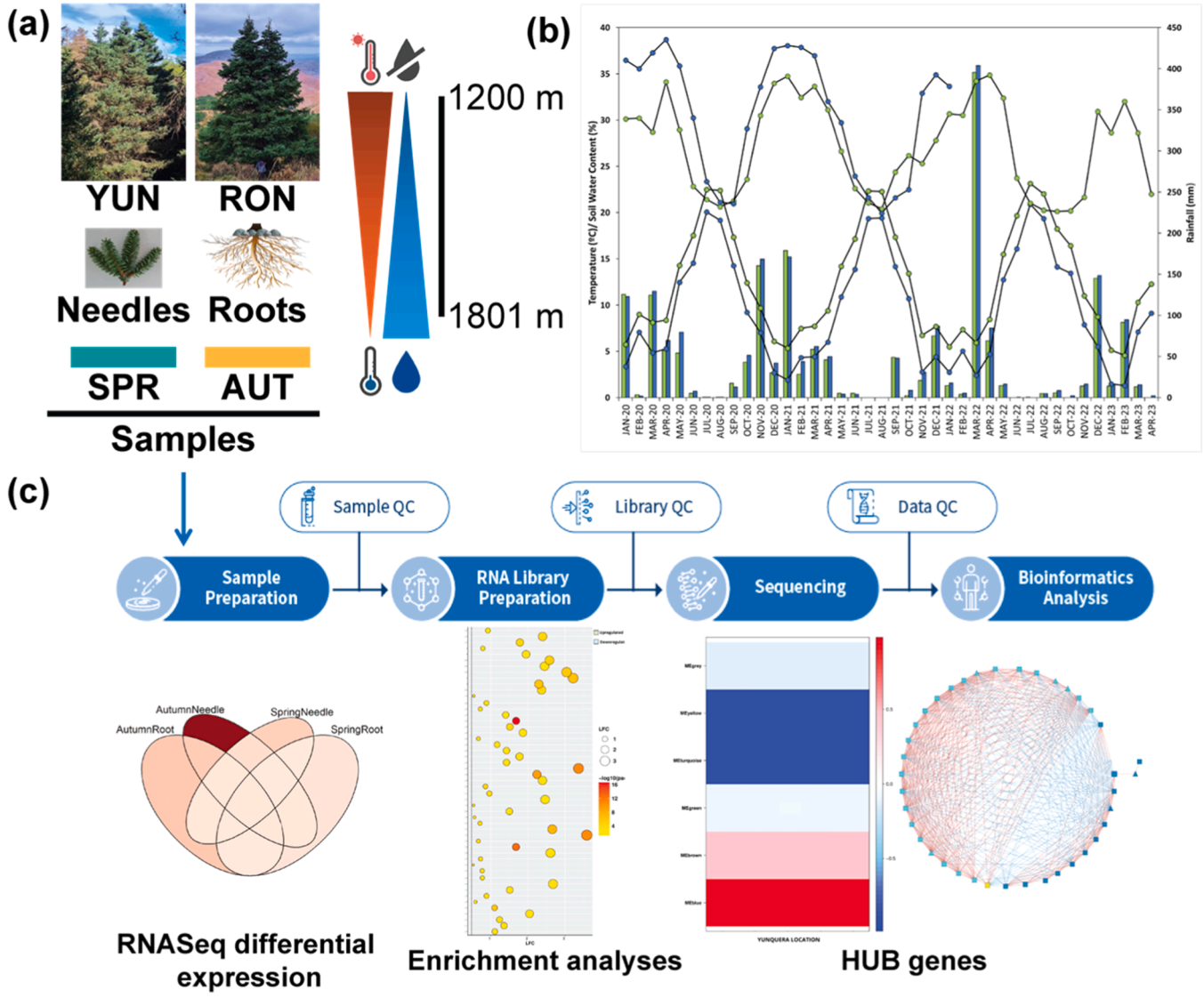

Fig. 1. Sampling sites, climatic parameters and experimental set-up for transcriptome analysis. (a) Two close but geographically distinct population of Spanish firs were studied: Yunquera (YUN) and Ronda (RON), located at different altitude and exhibiting differential climatic conditions. Needles and roots were harvested from adult trees growing in nature in spring (end of the rainy season) and early autumn (end of the dry season). (b) Profiles of temperature, soil water content and rainfall recorded in the sampling sites since January 2020 to April 2023, green circles (YUN), blue circles (RON). (c) Workflow followed for the comparative analyses of transcriptomes.

were ground in liquid nitrogen and extracted with the following buffer: 3 % (w/v) CTAB, 100 mM Tris pH 8.0, 2 M NaCl, 2 % (w/v) PVP40 and 30 mM ethylenediaminetetraacetic acid (EDTA). RNA purification was performed using lithium chloride as described (Canales et al., 2012). For RNA extractions from roots, the NucleoSpin RNA Plant kit (Cat. No. 740, 120.50, Macherey-Nagel, Düren, Germany) was used according to the manufacturer's instructions. Initial RNA quantification of the samples was performed using a NanoPhotometer N60 spectrophotometer (Implen) (Fisher Scientific, Leicestershire, UK), and sample purity was evaluated based on 260/280 and 260/230 ratios. RNA integrity was verified through agarose gel electrophoresis and further assessed using a Fragment Analyzer System with the Agilent DNF-472 HS RNA Kit (Agilent, CA, USA). Only samples with a RIN greater than 7 were included in subsequent analyses. cDNA synthesis was performed using 0.5 µg of total RNA and the iScript™ cDNA Synthesis Kit (Bio-Rad, Hercules, CA, USA), following the manufacturer's protocol. qPCR primers were designed in compliance with MIQE guidelines (Bustin et al., 2009), and their specifications are provided in Supplementary Table S1. Each qPCR reaction contained 10 ng of cDNA, 0.4 mM of primers, and 2X SsoFast™ EvaGreen® Supermix (Cat. No. 1725,204, Bio-Rad, Hercules, CA, USA), in a total reaction volume of 10 µL. Gene expression was quantified using the CFX 384™ Real-Time System thermocycler (Bio-Rad, Hercules, CA, USA). The qPCR program consisted of an initial denaturation step of 2 min at 95 °C, followed by 50 cycles of 1 s at 95 °C and 5 s at 60 °C. A melting curve analysis from 60 to 95 °C was included to confirm the specificity of the amplification. Data analysis was conducted as described by Cañas et al. (2014), using the MAK3 model in the R package qPCR (Ritz et al., 2008). Expression levels were normalized to the reference genes ap_1090: PSFP (peptidase S24/S26A/S26B/S26C family protein) and ap_2641: SLAP (Saposin-like aspartyl protease), previously validated for RT-qPCR experiments by Ortigosa et al. (2022). Each qPCR experiment included three biological replicates and three technical replicates per sample. Statistical differences in gene expression were analyzed using Past 4.03 software (Hammer et al., 2001).

2.3. Library construction and sequencing

Two types of libraries were prepared for the study: non-directional and directional. The non-directional library involved messenger RNA purification, RNA fragmentation, and first-strand cDNA synthesis using random hexamer primers, followed by second-strand cDNA synthesis with dUTP. For the directional library, dTTP was used for second-strand cDNA synthesis. All libraries were sequenced on an Illumina NovaSeq 6000 platform. A summary of sequencing metrics, including raw read counts, quality scores, read lengths, and the number of filtered reads, is presented in Table S2.

Raw RNA-seq reads were filtered for adapter contamination, reads with >10 % uncertain nucleotides and reads with >50 % low-quality bases. Sequencing was done twice, once in autumn and once in spring, at locations YUN and RON. Within each season, samples were prepared and sequenced together to eliminate technical batch effects.

For alignment, HISAT2 was employed, a sophisticated and sensitive alignment program known for its efficient mapping of next-generation sequencing reads. Due to the absence of a reference genome for *Abies pinsapo*, reference-based transcriptome alignment against the published transcriptome of *Abies pinsapo* by Ortigosa et al. (2022) was performed. A summary of mapping metrics, including alignment rates and uniquely mapped reads, is provided in Table S3. DNA sequencing was conducted by Novogene Corporation Cambridge, CB4, United Kingdom). These RNA-seq data have been deposited in NCBI's Gene Expression Omnibus (GEO) and are accessible under the GEO series accession number, GSE288980: https://www.ncbi.nlm.nih.gov/geo/query/acc.cgi?acc=GSE288980).

Transcript annotation was relied on the published transcriptome of *Abies pinsapo* by Ortigosa et al. (2022). These annotations were generated using BLAST2GO (Rokitta et al., 2005) using DIAMOND software with blastx option (Buchfink et al., 2021) against the NCBI's plants-nr database (Sayers et al., 2021). The annotation of genes of the LEA gene family was previously described in Blanca-Reyes et al. (2024) and the assignment criterion was by isoform appearance. However, in this transcriptomic analysis new isoforms appeared and were named in the same way and are detailed in the phylogenetic analysis in Figure S1.

2.4. Normalization and differential expression

To ensure robust and reliable comparisons between samples, a series of critical steps were undertaken to process the Novogene RNA count matrix (Figure S2). Differential expression analysis were performed separately for each season. Genes with exceedingly low expression levels across all libraries were filtered out by retaining only those with at least 10 normalized counts (DESeq2 baseMean) in a minimum of three samples following recommendations from the DESeq2 authors (Love et al., 2014). This threshold ensures that genes are expressed in at least half of the samples prior to further analysis. This essential filtering step mitigates the impact of statistical noise and reduces the multiple testing burden, thereby enhancing the sensitivity to detect differentially expressed genes. Differential gene expression analysis was performed to identify significant changes in gene expression between the two different locations, YUN and RON, using the *DESeq2* package for *R* (Love et al., 2014). Genes were considered differentially expressed if they had an adjusted p-value (padj) $\langle$ 0.05 and $|$ logFC$|$ $\rangle$ 0.5. Logarithmic fold change shrinkage was applied to refine the differential expression estimates. In all comparisons, RON was set as the reference population, such that positive log fold-change values indicate higher expression in YUN, and negative values indicate higher. expression in RON.

2.5. Functional enrichment analysis

Functional enrichment analysis was conducted using R to gain insights into the biological processes associated with the non-model organism, *A. pinsapo*. Gene IDs were mapped to GO terms based on the available annotations in the transcriptome (Ortigosa et al., 2022) as detailed in Table S4. Gene Ontology (GO) enrichment analysis was performed to identify significantly enriched terms among differentially expressed genes using the *topGO* package for *R* (v2.56.0, Alexa and Rahnenfuhrer 2024). GO enrichment analysis employed Fisher's exact test with the weight01 algorithm to account for the hierarchical structure of the GO terms.

2.6. KEGG enrichment analysis

KEGG pathway enrichment analysis was performed to identify significantly enriched pathways among differentially expressed genes. KEGG terms were annotated using both *KAAS* (Moriya et al., 2007) and *EGGNOG* (Huerta-Cepas et al., 2018) tools, ensuring comprehensive coverage of potential KEGG annotations.

Using the *clusterProfiler* package (Yu et al., 2012), KEGG pathway enrichment analysis was conducted. Pathways were considered significant if they met the criteria: a minimum gene set size of 5, and p-value and q-value cutoffs of 0.05. To focus on plant-specific pathways, the enrichment results were filtered using a predefined list of plant pathways.

2.7. Network construction

A weighted gene co-expression network was constructed using *WGCNA* (Langfelder and Horvath 2008). The soft thresholding power was selected to achieve a scale-free topology. Modules of co-expressed genes were identified, and their eigengenes were calculated to summarize the expression profiles of each module. Genes within the modules of interests were visualized to explore their expression patterns. Hub genes, defined as highly connected and central within their respective modules, were identified based on correlation measures. Specifically, genes were considered hub candidates if they exhibited strong correlations ($|corr| > 0.5$) with the trait of interest (the geographical locations YUN and RON) and had high module membership (MM > 0.8; Li et al., 2020). The selected hub genes were visualized using *Cytoscape* (Shannon et al., 2003).

2.8. Phylogenetic analysis

Phylogenetic analysis of arogenate dehydratase (ADT) was performed including protein sequences from *Pinus pinaster* (Pp), *Arabidopsis thaliana* (At) and *Abies pinsapo* (ap). Sequences corresponding to type I (green) and type II (yellow) ADTs, as described in El-Azaz et al. 2022, are highlighted in bold. The analysis was performed after a Muscle type alignment and following the Maximum Likelihood method with 1000 bootstrap replicates.

For the phylogenetic analysis of LEA proteins, sequences from *Pinus taeda* (Pta), *Arabidopsis thaliana* (At) and *Abies pinsapo* (Ap) were included, as well as sequences corresponding to LEA from group D of different conifer species including *Picea glauca, Picea abies, Abies pinsapo* (Ap), *Abies alba, Abies balsamea*, *Pinus taeda* (Pta), *Pinus pinaster, Pinus nigra, Pinus halepensis, Taxus baccata* and *Cryptomeria japonica*. The analyses were performed after ClustalW type alignment and following the Maximum Parsimony method with 1000 bootstrap replicates. All phylogenetic analyses were performed using MEGA-11 software (Tamura et al., 2021). All sequences used are listed in Table S2.

2.9. ApLEA30 cDNA cloning

Full-length cDNA for ApLEA30 was isolated from *Abies pinsapo* tissue using specific primer pairs detailed in Table S1. cDNA was subcloned into the pJET1.2 vector (ThermoFisher Scientific, Waltham, MA, USA). The full-length cDNA was then amplified via PCR using forward and reverse primers containing attB1 and attB2 sites at their 5′ and 3′ ends, as described in Table S1. The amplified product was first cloned into the

pDONR207 vector. Subsequently, *ApLEA30* was transferred into the pDEST17 vector using BP Clonase® II and LR Clonase® II enzyme mixes (Thermo Fisher Scientific, Waltham, MA, USA).

2.10. Subcellular localization

The predicted signal peptide of ApLEA30 [MAAFSAKMPVLSKGSTCPGLTAMRSTTVASKTNRVCFRAIARAG] was cloned into the pGWB5 vector using Gateway technology (Thermo Fisher Scientific, Waltham, MA, USA), resulting in GFP-tagged signal peptide at their C-termini under the control of the CaMV 35S promoter. These constructs were introduced into *Agrobacterium tumefaciens* C58C1 strains via electroporation. GFP-tagged signal peptide production was induced in *Nicotiana benthamiana* leaves through agroinfiltration at an OD600 of 0.5, following established protocols (He et al., 2004). In all experiments, the p19 silencing suppressor was co-expressed (Garabagi et al., 2012). GFP fluorescence was analyzed 48 h post-agroinfiltration using a Leica Stellaris 8 confocal microscope (Leica, Wetzlar, Germany). Chloroplast autofluorescence was observed using excitation/emission wavelengths of 488/680–700 nm, while GFP detection used 488/505–525 nm, powered by a 488 nm argon ion laser. Protein expression was validated by western blot analysis.

To grow *N. benthamiana* plants for this experiment, seeds were initially in shared pots for 1–2 weeks and later transplanted into individual pots for an additional 3–4 weeks. Seedlings were maintained at 25 °C in a growth chamber with 16-hours of light/8-hours of dark photoperiod.

2.11. Recombinant expression and salt treatment in E. coli

The ApLEA30 DNA sequence, excluding the predicted transit peptide, was subcloned into the pDEST17 vector using Gateway technology. The pDEST17 construct was introduced into *Escherichia coli* BL21-CodonPlus-RIL® cells (Agilent Technologies, Santa Clara, CA, USA). Cultures were grown in 25 mL of LB medium supplemented with 100 μg/mL ampicillin and 34 μg/mL chloramphenicol at 37 °C until an OD600 nm of 0.5 was reached. Protein expression was induced with 1 mM IPTG, followed by 2 h of incubation at 37 °C with gentle shaking (100 rpm).

Salt treatment experiments followed the protocol described by Gao and Lan (2016). Two hours after induction with IPTG, cultures were adjusted to the same optical density and 5 μL of serial dilutions were spotted onto LB plates containing varying NaCl concentrations (171, 300, 400, 500, 600, and 700 mM). Plates were incubated overnight at 37 °C.

2.12. Protein extraction, SDS-PAGE, and immunodetection

Total proteins were extracted from plant material using a buffer containing 100 mM Tris (pH 8.0), 10 % (v/v) glycerol, 1 % (w/v) sodium dodecyl sulfate (SDS), 2 mM EDTA, and 0.1 % (v/v) beta-mercaptoethanol. For protein extraction from *E. coli* cell cultures, an extraction buffer composed of 100 mM Tris, 2 mM EDTA, 10 % glycerol and 0.5 mM PMSF was used.

Approximately 100 mg of frozen plant material or the pellet from 1 mL of cell culture were resuspended in 100 μL of the buffer at room temperature. Intact chloroplasts were isolated using the CPISO chloroplast isolation kit (Merck, Darmstadt, Germany) in combination with a Percoll® gradient. After centrifugation at 20,000 × *g* for 10 min at 4 °C, 75 μL of the supernatant was mixed with 25 μL of 4 × Laemmli buffer and denatured at 100 °C for 5 min. Proteins (25 μg) were separated by SDS-PAGE and analyzed by western blot using a GFP-specific commercial antibody (GFP (B-2), mouse monoclonal antibody, Santa Cruz Biotechnology, Santa Cruz, CA, USA) at a 1:1000 dilution.

2.13. Extraction and quantification of total flavonoid content

Total flavonoid content in *A. pinsapo* needles and roots was extracted and quantified following Rossi et al. (2022). Frozen ground tissue (250 ± 2.5 mg) was extracted in 1.3 mL of 70 % methanol (CAS 67–56–1, VWR, product no BDH1135). After vortexing for 1 min, samples were centrifuged at 6700 × *g* for 10 min at 20 °C. The supernatant was transferred, and the pellet was resuspended in 1.5 mL of solvent, vortexed for 1 min, and centrifuged again at 7200 × *g* for 10 min at 20 °C. The process was repeated to ensure efficient extraction. Supernatants were pooled, centrifuged at 7200 × *g* for 10 min at 20 °C and stored at −80 °C for phenolic compounds analysis.

In a 96-well microplate wells (Greiner Bio-One, flat-bottom, clear, 655,101), 70.4 μL of deionized water (DI H_2O), 24 μL of diluted sample extract (1:5) or a standard solution of catechin ($C_{15}H_{14}O_6 \cdot xH_2O$, CAS 225,937–10–0, Sigma-Aldrich, product no C1251) were dispensed, using DI H_2O (as a blank). Sequentially, 20 μL each of sodium nitrate ($NaNO_2$, 18 g/L, CAS 7632–00–0, Sigma-Aldrich, product no S2252), 20 μL of aluminum chloride hexahydrate ($AlCl_3 \cdot 6H_2O$, 65 g/L, CAS 7784–13–6, Sigma-Aldrich, product no 237,078), 48 μL of sodium hydroxide (NaOH, 1 M, CAS 1310–73–2), and 57.6 μL of deionized water were added.

Absorbance at 510 nm was measured 10 min after NaOH addition using a microplate reader. Total flavonoid content (expressed in mg/L) was quantified as catechin equivalents (Cat. eq) based on a calibration curve.

3. Results

3.1. Needle gas-exchange in mid-spring and early-autumn in A. pinsapo trees from the lower and upper ecotones

In mid-spring (May, warm and wet conditions, peak of the growing season), no significant differences in net photosynthesis and stomatal conductance rates were found between the two studied populations (Fig. 2). Contrastingly, by the end of the dry dormant-season (AUT), gas-exchange rates were significantly different at the two populations (upper (RON; 1700–1800 m asl) and lower (YUN; 1100–1200 m asl). While trees at YUN showed almost complete stomatal closure and therefore near zero net photosynthesis, the trees at RON showed comparatively high stomatal conductance rates allowing for C assimilation rates that were about eight times higher than in YUN. This indicates highly stressful, water-limitation conditions at the lower ecotone and a compromised carbon balance in the trees during the dry season. However, even at the moment of the year of maximum water-stress, the upper ecotone population cope to maintain relatively high net assimilation rates, more than a half those observed at the peak of the growing season. These results indicate that YUN population was more negatively impacted when growing in its natural distribution.

3.2. Comparing the transcriptomes of A. pinsapo forests

To examine the molecular basis underlying the observed differences in physiology, the transcriptomes of needles and roots of trees located in YUN and RON were compared, using RON as a reference population with better physiological performance (Table 1). A large number of genes (2331) were differentially expressed in needles at the end of the dry season (autumn), with more genes being down-regulated genes (1271) than up-regulated (1060). The change between both transcriptomes was much lower at the peak of the growing season (spring), when the total number of differentially expressed genes (DEGs) was of only 289, and a similar proportion of down- and upregulated genes was observed. When the root transcriptomes from RON and YUN were compared, the total number of DEGs was lower than in needles overall. However, in roots, the number of DEGs was markedly higher in autumn (518) than in spring (67), reflecting a stronger transcriptomic response

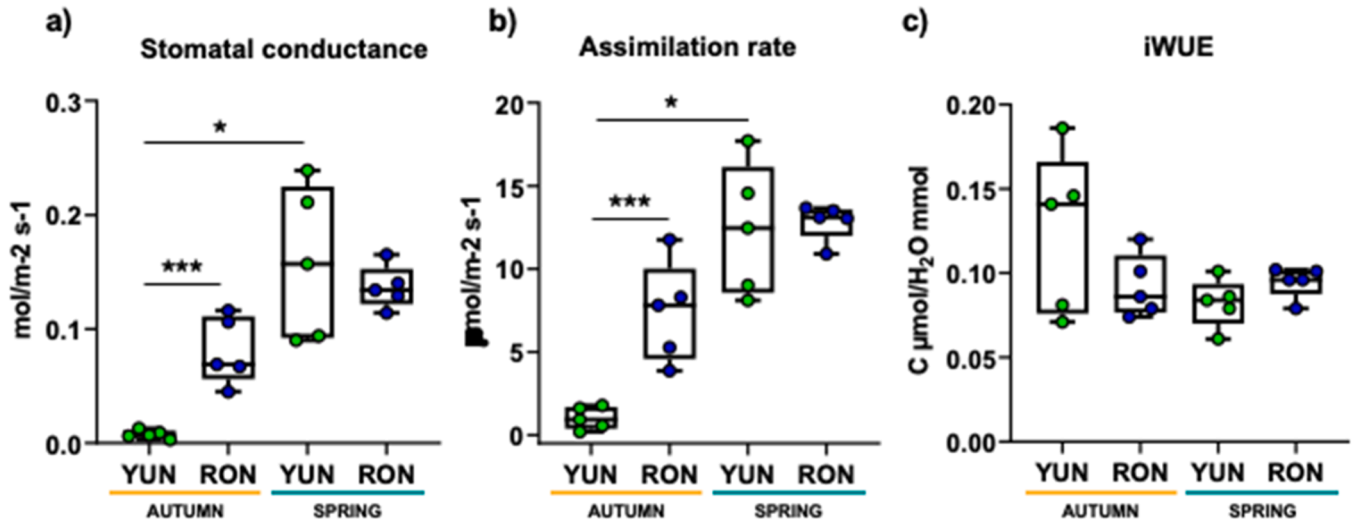

Fig. 2. Field-measured, *A. pinsapo* physiological parameters (needle gas-exchange rates). Stomatal conductance (a) and carbon assimilation (b) rates at the YUN and RON populations in spring (SPR; peak of the growing season) and early Autumn (AUT; end of dry, dormant season). Calculated values of intrinsic water use efficiency (iWUE) are shown in (c). Statistical analysis was performed using a Mann-Whitney *U* test, statistically significant differences are marked with asterisks (*p-value<0.05, ** p-value<0.01, ***p-value<0.001).

Table 1
Differentially expressed genes in needles and roots of YUN trees using RON as a reference.

Condition	Total	Upregulated	Downregulated
Autumn Needle	2331	1060	1271
Autumn Root	518	280	238
Spring Needle	289	153	136
Spring Root	67	45	22

to environmental stress in autumn. Despite the similar spring-to-autumn DEG ratios observed in both tissues, the absolute number of responsive genes remained consistently lower in roots than in needles (Fig. 3a). Notably, a remarkable number of DEGs (217) were found in common between the transcriptomes of needles and roots of trees that were sampled at the end of the dry period, after a prolonged period of water shortage and hot temperatures in the forest. In contrast, the number of DEGs in common between needles and roots from trees sampled in spring at both locations was extremely low (3), suggesting a negligible effect of adverse environmental factors on the transcriptome dynamics at the end of the rainy period.

Co-expression analyses of DEGs were performed to identify potential patterns of transcriptional activity that could be linked to the response of *A. pinsapo* against environmental stress factors. Hierarchical clustering was applied to DEGs identified across all samples, combining both tissue types (needles and roots) and seasons (spring and autumn) to capture broader expression patterns associated with seasonal shifts and tissue identity (Fig. 3b). This analysis includes both needles and roots sampled in spring and autumn to capture broader expression patterns associated with tissue identity and seasonal response. As shown in the heatmap, the global profiles of DEGs in needles and roots were quite different when samples from spring and autumn were compared, indicating a seasonal readjustment of co-expressed genes in the transcriptome. In needles, most upregulated genes were clustered in distinct groups and subgroups, while in roots, both upregulated and downregulated DEGs were mainly associated with a single module (Fig. 3b, compare needles and root columns in autumn). A detailed list of DEGs in needles and roots from YUN trees during autumn and spring is presented in Table S5 (supporting information).

3.3. Technical validation of transcriptomic data

The transcriptomic data shown in Table 1 and Fig. 3 were validated by quantitative determination of the expression of selected representative genes (Figure S3). Transcript levels for 12 different genes were analyzed using RT-qPCR in the same biological samples (from needles and roots of trees from each location) in which the RNA-seq was performed, including three technical replicates per sample. Overall, the expression levels determined by RT-qPCR matched those derived from RNA-seq. Thus, the expression of *ApLEA30* (ap-2991), and a NAC transcription factor (TF) (ap-28,951) were significantly upregulated in needles and roots by the end of the dry season (autumn onset). Conversely, transcript abundance of *ADT* (ap-6413), *phospho-2-dehydro-3-deoxyheptonate aldolase* (ap-71,257) and *chalcone synthase* (ap-4904) were downregulated in the same samples. The expression of *ApLEA30* (ap-2991), *WAT1-related protein* (ap-12,775) genes and transcripts encoding a NAC (ap-28,951) were also upregulated in the samples harvested in spring. It should be noted that the number of upregulated and downregulated transcripts was much lower in these samples in comparison to the trend observed in early autumn, consistently to what was found in the global transcriptomic analysis previously performed (Table 1 and Fig. 3).

3.4. Identification of structural and regulatory genes responding to climate stress

To gain insights into the identity of DEGs and the specific biological processes they are involved in, a functional enrichment analysis was performed using TOPGO (see Materials and Methods section and Figure S4). Fig. 4 summarizes the results obtained from the needles and roots of YUN and RON trees sampled in autumn, the most stressful season under study. Several biological processes and metabolic pathways, such as response to water stress, flavonoid biosynthesis, secondary cell wall transport and thickness of wood fibers, and aromatic amino acid biosynthesis, were affected. Genes involved in these processes were differentially expressed, with some being upregulated and others downregulated. Additionally, several transcription factors (TFs) potentially involved in the regulation of the above-mentioned processes were also found to be differentially expressed.

In needles, one of the biological functions enriched in the GO analysis was response to stress (Fig. 4, needles, right panel). Transcripts

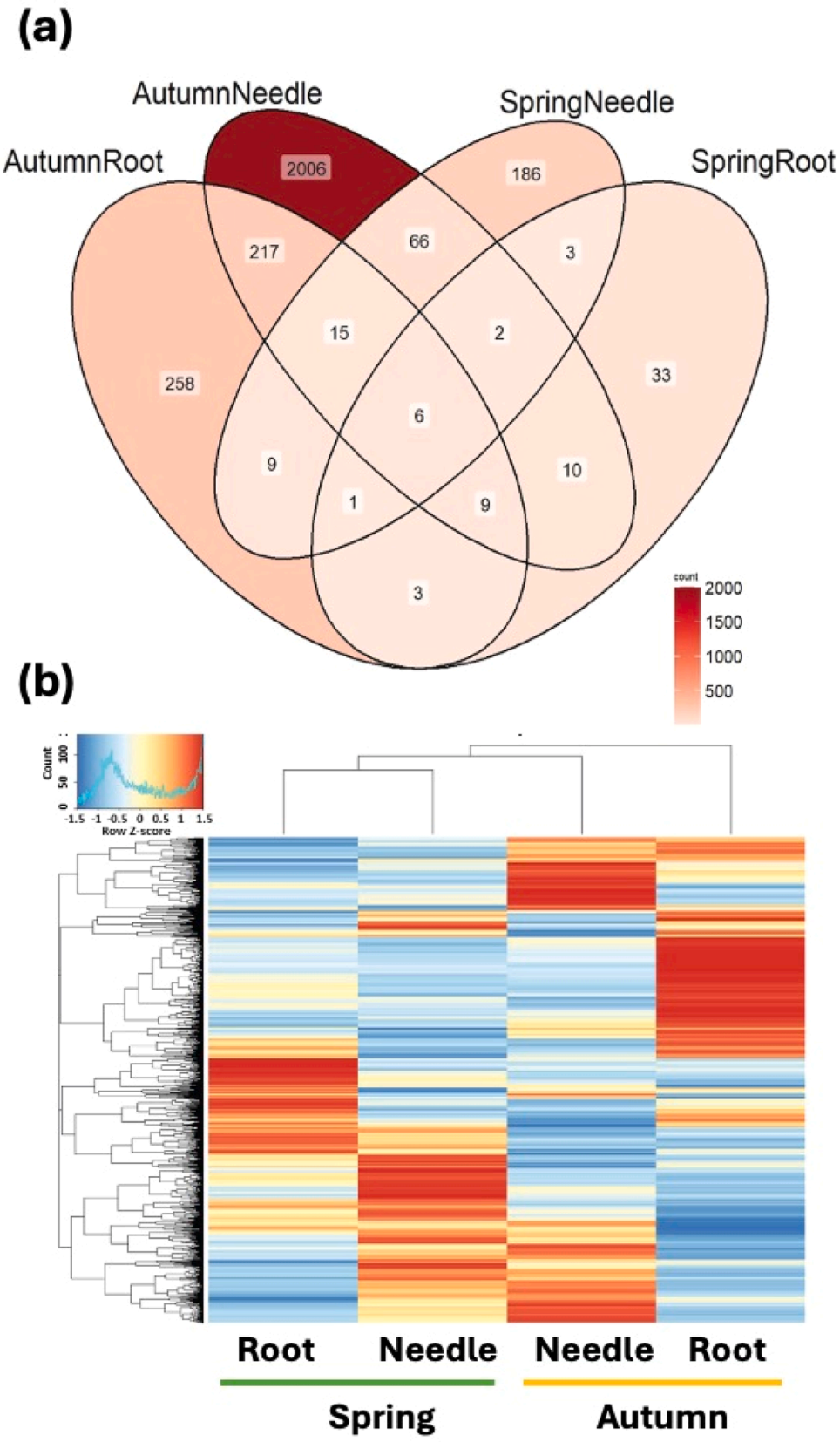

Fig. 3. Differential expression analysis, using RON as the reference population. Venn diagrams of genes differentially expressed in samples from needles and roots harvested in spring and autumn (a). Hierarchical clustering and heat map of DEGs from needles and roots harvested in spring and autumn (b).

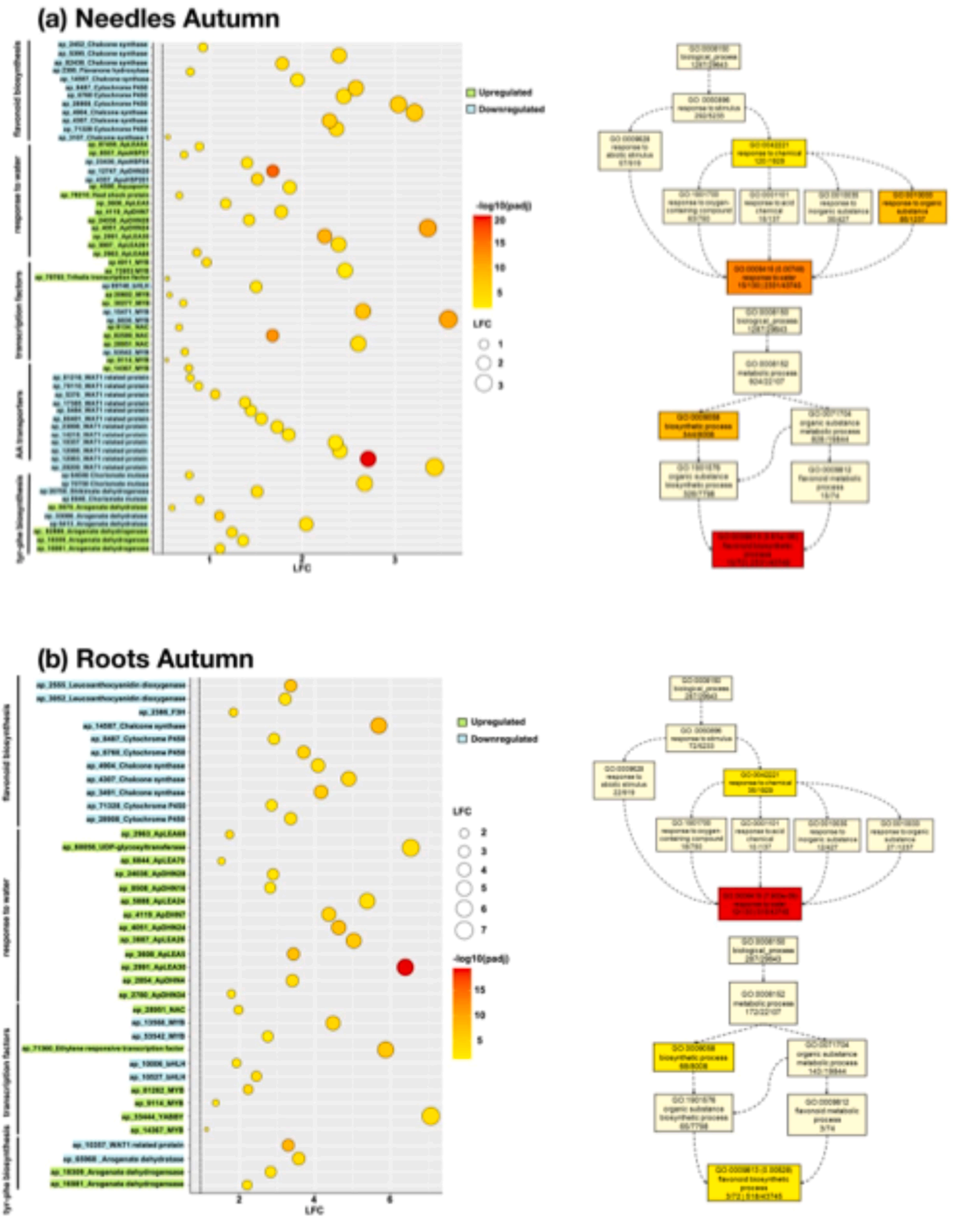

Fig. 4. Comparative dynamics of the Spanish fir transcriptomes in response to environmental stress. Left panel, graphical representation of DEGs according to their relative abundance (LogFC) and statistical significance (-log10padj) and their links to different biological processes and metabolic pathways. Right panel, biological processes significantly enriched in the GO analysis. Dynamics of the needle (a) and root (b) transcriptomes.

upregulated in YUN versus RON trees included several members of the Late Embryo Abundant (LEA) protein family, with *ApLEA26* and *ApLEA30* being particularly overexpressed and exhibiting the highest LogFC values (Fig. 4, needles, left panel). Transcripts for several members of the dehydrin (DHN) group, such as *ApDHN20* and *ApDHN24* were also upregulated. Conversely, downregulated genes included those encoding aquaporin and other stress-related proteins, such as small heat shock proteins (ApsHSP20 and ApsHSP24). In roots, members of the LEA (*ApLEA24, ApLEA26 and ApLEA30*) and DHN (*ApDHN7* and *ApDHN24*) families again showed the highest levels of differential expression, with much elevated LFC values than those observed in needles (Fig. 4b, roots, left panel).

In the KEGG analysis, flavonoid biosynthesis was a significantly enriched metabolic pathway among downregulated transcripts in the needles of YUN trees (Fig. 4a, needles, right panel), including chalcone synthase and flavanone hydroxylase genes (Fig. 4a, needles, left panel). Similar genes were also downregulated in roots, although their LogFC values were substantially higher than in needles (Fig. 4b, roots, left panel). Furthermore, in roots, additional transcripts for genes involved in flavonoids biosynthesis, such as anthocyanidin dioxygenases, were also downregulated, suggesting a major impact of stressful conditions on this organ (Fig. 4b, roots, left panel).

Numerous transcripts for WAT1-related protein were also downregulated in needles (Fig. 4, needles, left panel). WAT1 is a transmembrane protein involved in secondary cell wall formation in wood fibers. In Arabidopsis, WAT1's biological role is linked to indole metabolism and tryptophan/auxin transport Ranocha et al. (2010). Interestingly, the differential expression of WAT1 was much less pronounced in roots, suggesting a minor alteration in its function in this organ during the end of the dry season (autumn).

The biosynthesis of aromatic amino acids was another metabolic function altered by environmental stress in the *A. pinsapo* populations (Fig. 4, left panel). In both needles and roots, genes for *ADT* were downregulated, while those encoding arogenate dehydrogenases (*ADH, TyrA*) were upregulated in YUN trees growing under stressful conditions (autumn). Consistent with the observed lower abundance of *ADT* transcripts, additional genes in the shikimate pathway were also downregulated in needles. However, an exception to the above-mentioned pattern of gene expression was the transcript ap-5675 (*ADT*) that was upregulated in needles (Fig. 4, needles, left panel).

Finally, the functional enrichment analysis differentially expressed genes encoding TFs that could be involved in the transcriptional regulation of the biological processes described above (Fig. 4, left panel). Various transcripts for members of the MYB, NAC and bHLH families were upregulated or downregulated in needles and roots from YUN trees harvested in autumn. Additionally, a *Trihelix* family gene was upregulated in needles, while members of the *ERF* and *YABBY* gene families were exclusively upregulated in roots (Fig. 4, left panel, compare TFs in needles and roots).

3.5. Searching for regulatory gene networks governing Spanish fir responses to climate stress

To further investigate the molecular basis of the transcriptome dynamics observed in contrasting populations of Spanish firs, we identified genes exhibiting an enhanced level of interactions within and between co-expression modules. The top 10 % of the transcripts with the most interactions were considered as hub genes. Using this criterion, hierarchical clustering of these hub genes established relationships between modules and expression in needles and roots of YUN trees sampled in autumn after a long period of dryness and high temperatures. The modules are color-coded for convenience, with each module containing genes that exhibit highly correlated expression profiles across samples, suggesting shared regulatory control or biological function (Saelens et al., 2018). As shown in the heatmap of Fig. 5 (right panel), the yellow and the turquoise modules exhibited similar levels of negative correlation with global expression in needles, while the blue module showed the highest positive correlation. In roots, the turquoise module was also negatively correlated with global gene expression; however, the highest values of positive correlation in this organ were found in the yellow and blue modules. Modules were selected based on their eigengene correlation with the trait "YUN vs RON," which serves as a proxy for the location of interest. Modules with significant correlations ($p < 0.05$) were prioritized for further functional interpretation (De Silva et al., 2022).

A network diagram was constructed to show hub genes with the most connections in the needles of YUN trees (Fig. 5, needles, left panel). An extremely complex gene co-expression network points out interactions of stress-related proteins such as the specific interactions of ApLEA1 and ApLEA30 with the regulatory genes NAC25. When a similar gene co-expression analysis was accomplished for relevant hub genes in roots of the same trees (Fig. 5, roots, left panel), a well-defined gene network was identified that included upregulated hub genes of the blue and yellow modules. These genes encode stress-related proteins of the LEA (ApLEA5, ApLEA24, ApLEA26, ApLEA30) and DHN (ApDHN4, ApDHN7, ApDHN16, ApDHN24. ApDHN28) families, enzymes involved in the biosynthesis of aromatic amino acids (ADH2), and TFs such as NAC25, ERF061 and YABBY5. Interestingly, again ApLEA30 and ADH2 showed a key position in the network exhibiting a high level of connectivity with multiple interactions.

3.6. Molecular and functional characterization of ApLEA30

Response to water stress was one of the most relevant biological responses identified in the transcriptomic comparison between YUN and RON populations. As *ApLEA30* appears to be a relevant hub gene involved in the response of YUN trees to environmental stress at the end of the dry period, it was selected for further investigation of its functional properties and subcellular location (Fig. 6). The sequence for *ApLEA30* was retrieved from the *A. pinsapo* transcriptome database (Ortigosa et al., 2022) and PCR-amplified using specific primers (Table S1). The full-length cDNA was recombinantly expressed in *E. coli* to overproduce an 18 kDa polypeptide, consistent with the estimated size defined by the ORF of the DNA sequence (Fig. 6, right panel, a). Given that high salt levels result in lower osmotic potential, which restricts water availability, the function of ApLEA30 in response to water stress was studied in *E. coli*. Bacterial cells overexpressing the recombinant protein were subjected to increasing concentrations of salt, following the experimental conditions described by Gao and Lan (2016). Fig. 6 (right panel, b) shows that cells transformed with the ApLEA30 construct showed significantly enhanced cell viability compared to those transformed with the control vector.

To determine the subcellular location of ApLEA30, the predicted signal peptide (cloned as described in Materials and Methods) from the full-length cDNA was fused to GFP and agroinfiltrated into *N. benthamiana* leaves. The transiently expressed construct for ApLEA30 revealed strong fluorescence labelling associated with chloroplasts, which were easily identifiable in photosynthetic cells by the chlorophyll autofluorescence (Fig. 6, left panel, GFP). Merged images visualized yellow labelling, corresponding to the co-localization of chlorophyll and ApLEA30 within the plastids. Magnified images unequivocally confirmed the plastid localization of ApLEA30.

3.7. Functional insights into the biosynthesis of aromatic amino acids and the metabolism of flavonoids in stressed Spanish fir

Transcriptomic analyses revealed that increased temperature and drought triggered metabolic changes in the pathways involved in aromatic amino acid and flavonoid biosynthesis. To understand how these changes integrate into the response to climate stress, flavonoid contents were determined in the needles of the same trees. Fig. 7a shows that flavonoid levels were significantly lower in YUN than in RON

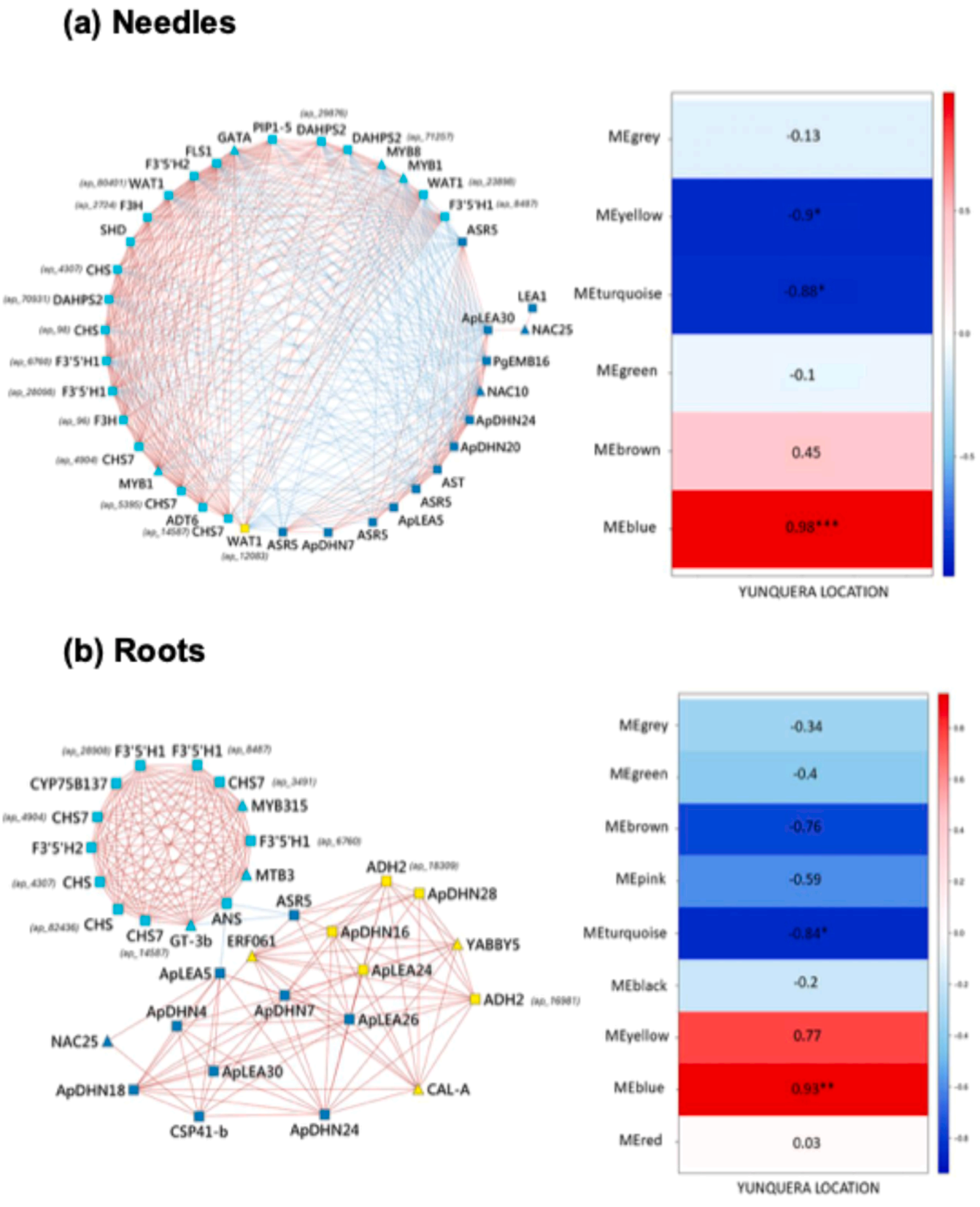

Fig. 5. Hub genes exhibiting differential expression in the YUN population. Heat maps and co-expression network interactions of hub genes differentially expressed in needles (a) and roots (b).

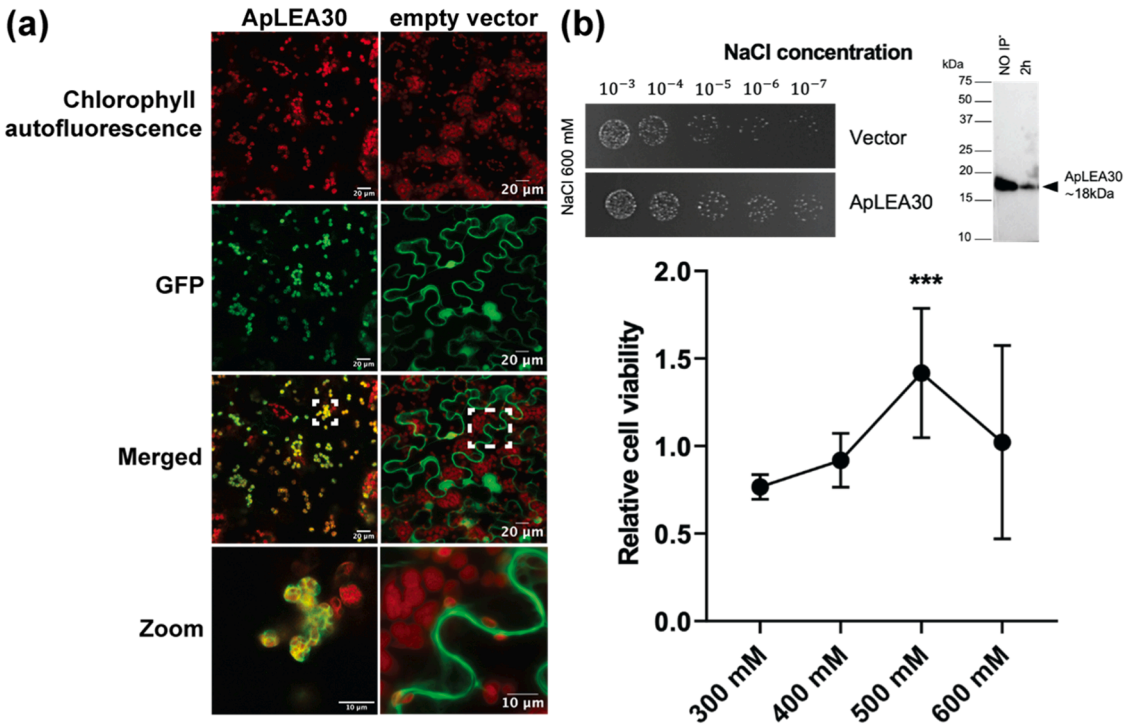

Fig. 6. Localization and functional validation of the candidate gene *ApLEA30*. Left panel, subcellular localization of the ApLEA30 protein in the plastids. Right panel, recombinant overproduction of ApLEA30 protein (a) and assays of cell tolerance to salinity stress (b). The data were initially analyzed using a Kruskall–Wallis test, and subsequently, upon identifying significant differences, a multiple comparisons test (Dunn posthoc) was performed. Statistically significant differences are marked with asterisks (****p-value*<0.001).

populations when samples were harvested in early autumn, at the end of the dry season. However, no major differences were found when samples were harvested in spring, at the end of the rainy period. Interestingly, the expression levels of *ADT*-type II were also lower in YUN than in RON locations at the end of the dry season meanwhile transcript abundance of ADT-type I was similar at both locations (Fig. 7b). ADT catalyzes the biosynthesis of phenylalanine, a precursor for the biosynthesis of flavonoids. In contrast, a concomitant upregulation of *ADH* transcripts, encoding an enzyme involved in the tyrosine biosynthesis, was observed. These results strongly suggest a shift in the channeling of aromatic amino acids as precursors for the biosynthesis of alternative secondary metabolites in response to environmental stresses.

4. Discussion

Rising temperature and decreasing rainfall are key factors inherent to climate change, resulting in prolonged periods of drought in many forest ecosystems. Mediterranean forests are especially vulnerable to these environmental disturbances, with populations locally adapted to different microclimatic environments (Sánchez-Salguero et al., 2017). This is the case of the YUN and RON populations located in the "Sierra de las Nieves" National Park (Fig. 1). In a previous work, the seasonal expression patterns of genes associated with the response to increased temperature and water stress were explored to define potential differences between Spanish fir populations. It was found that expression of stress-related genes was greater in trees growing under more stressful local climatic conditions (Blanca-Reyes et al., 2024), confirming previous ecophysiological studies showing that these populations were more vulnerable to the effects of climate change (Linares et al., 2012). In the present study, a holistic approach was accomplished to further understand how environmental disturbances influence transcriptome modulation. To confirm previous molecular data and substantiate the transcriptomic analyses, physiological parameters were assessed in the field using the same individuals sampled for molecular profiling. In autumn, at the end of the dry season, transpiration rates and stomatal conductance were significantly lower in trees growing at lower altitude (YUN) than in those growing at higher altitude (RON). Since stomatal conductance is influenced not only by stomatal aperture but also by stomatal density (Lawson and Vialet-Chabrand 2019), the observed differences suggest that environmental conditions may be affecting stomatal development and behaviour. This adjustment likely represents a strategy to optimize gas exchange while water loss under stress (Fig. 2). In contrast, differences between both populations were much smaller in spring. Taken together, the results demonstrate decreased photosynthetic capacity during the summer in trees growing at the more vulnerable (YUN) location, reflecting a major impact of the unfavourable environmental conditions on their physiological status.

4.1. *Effect of climatic stress on the Spanish fir transcriptome*

To identify metabolic pathways and gene networks affected by the environmental stresses, the transcriptomes of both populations subjected to contrasting climatic conditions were compared, using the RON population as a reference (Fig. 1). The transcriptomes of needles and roots from YUN trees were more substantially altered in autumn than in spring, indicating a major effect of the water shortages and high temperatures during the dry season (Fig. 3). Interestingly, although the total number of DEGs was much higher in needles (2331) than in roots (518), a greater proportion of genes were upregulated in roots, suggesting tissue-specific transcriptional strategies in response to environmental stress (Fig. 3). Previous transcriptomic studies in various conifer species have been undertaken to evaluate responses to water stress (de María et al., 2020; Haas et al., 2021; Manjarrez et al., 2024a, 2024b), including *A. pinsapo* saplings (Cobo-Simón et al., 2023). Overall, the number of DEGs reported in these studies is higher than that observed in the present work. However, it is difficult to have these works as a reference for the present study because the experimental approaches were accomplished under controlled conditions of growth. In contrast, all

(a)

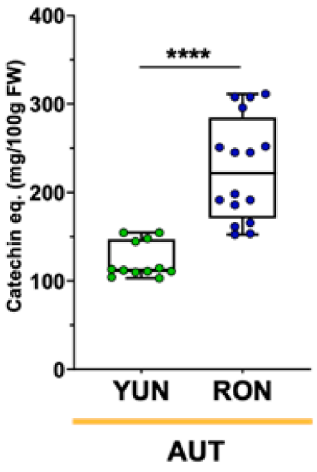

Total flavonoid content		
Location	YUN	RON
Mean	123.29	226.03
SD	20.42	58.24
N	12	16
pvalue	<0.0001	

(b)

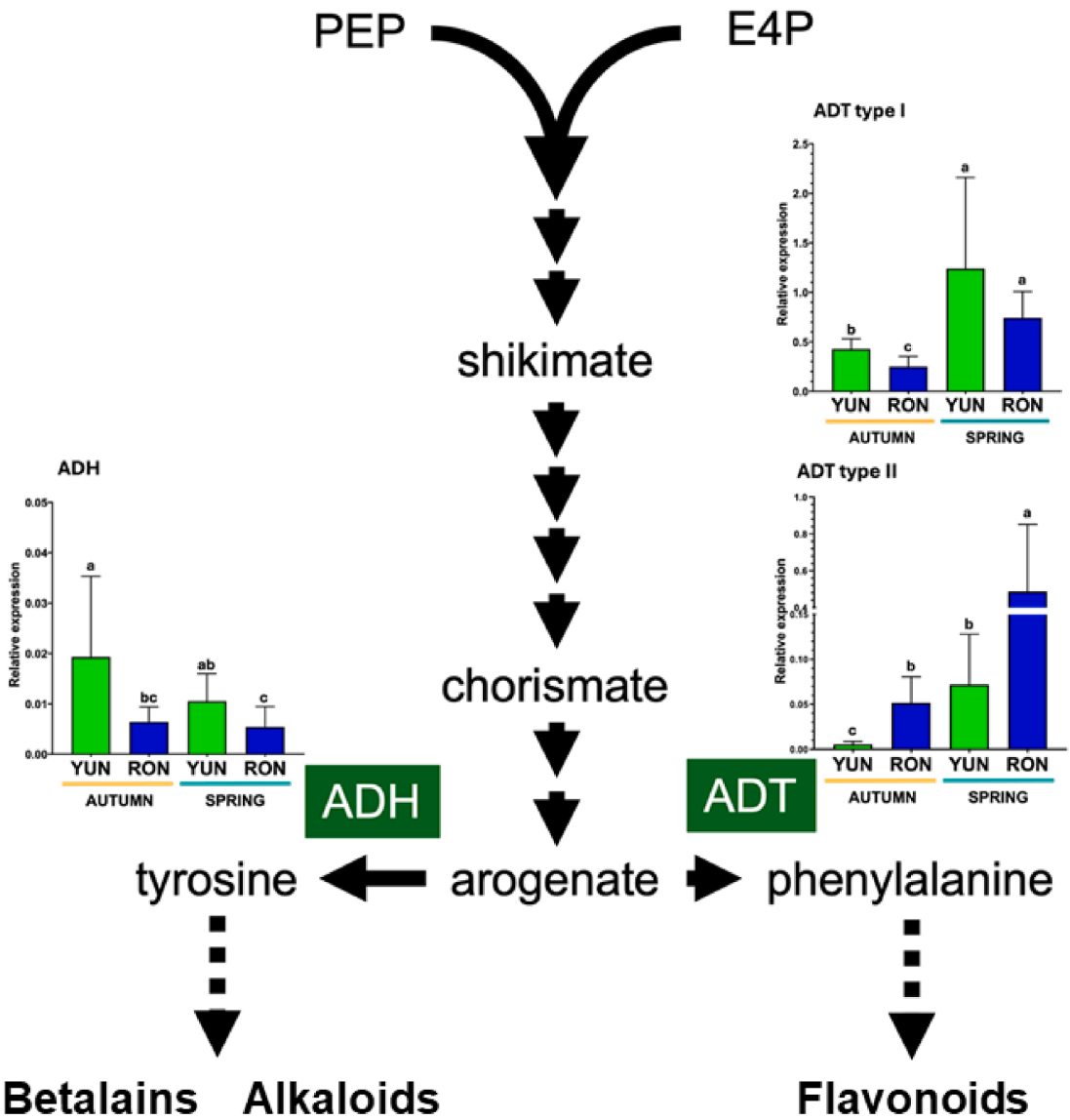

Fig. 7. Secondary metabolite pathways, (a) Flavonoids contents and (b) transcript expression levels of ADT and ADH in the YUN and RON populations. PEP, phosphoenolpyruvate; E4P, eritrose-4-phosphate. Statistical analysis of flavonoids content was performed using a Mann-Whitney *U* test, statistically significant differences are marked with asterisks (****p-value<0.0001). The qPCR results were first examined using the Kruskal-Wallis test. When significant differences were found, a Dunn's post hoc test was conducted for multiple comparisons. Distinct letters represent statistically significant differences.

measurements presented here have been performed on trees growing in their natural habitats and subjected to environmental changes occurring under the effects of current climate change. Furthermore, modifications in the transcriptome were investigated in a variety of samples such as seedlings (Haas et al., 2021), clonally propagated cuttings (Fox et al., 2018), scion and rootstock stems (Manjarrez et al., 2024a, 2024b), instead of in adult trees growing in natural conditions, as in this study.

4.2. Upregulation of stress-related proteins in response to water stress and increased warming

Responses to water stress were particularly enriched in the transcriptomic analysis. Several genes of the large family encoding Late Embryogenesis Abundant (LEA) proteins, including those in group II, also called dehydrins, were upregulated in YUN trees at the end of the dry period in both needles and roots. However, the number of upregulated genes encoding these stress-related proteins, as well as the relative abundance of the corresponding transcripts, was much higher in roots (Fig. 4). These findings align with those reported in a previous study in which the relative expression levels of selected genes were compared (Blanca-Reyes et al., 2024). LEA proteins are well-established as protectors of plant cells against deleterious effects triggered by abiotic stresses, including drought (Hincha and Thalhammer 2012). Moreover, it has been suggested that the expansion of dehydrins in the Pinaceae could be related to increased tolerance to water stress in this plant lineage (Sena et al., 2018).

Conifers in areas with Mediterranean-type climate are generally more resilient to water stress than those in temperate regions. However, their recovery potential may be constrained by the recurrent dry periods suffered in the recent years (Gazol et al., 2018).

Downregulation of flavonoid biosynthesis: is flavonoid abundance a response to climatic-stress under field-conditions

Several transcripts involved in phenylalanine biosynthesis were downregulated in needles and roots of the YUN population (Fig. 4). These include genes encoding shikimate dehydrogenase, chorismate mutase and ADT, which are coordinately regulated in plants (Corea et al., 2012a, 2012b). ADT catalyzes the last and rate-limiting step of phenylalanine biosynthesis and is encoded by a large gene family consisting of at least 9 members in conifers, which are involved in the biosynthesis of phenylalanine for distinct metabolic fates (El-Azaz et al., 2016; Pascual et al., 2016). Two types of ADT enzymes have been described in plants: ADT-type I, which are allosterically inhibited by phenylalanine, and ADT-type II, which are deregulated. Several genes encoding ADT-type II are essential for the biosynthesis of high phenylalanine levels, which can subsequently be channeled into the lignin biosynthesis in conifers (El-Azaz et al., 2020, 2022). Interestingly, the *ADT* transcripts downregulated in *A. pinsapo* are unrelated to the late-mentioned genes and appear to be orthologous of Arabidopsis *ADT-6*, a member of the gene family that is specifically involved in flavonoid biosynthesis (Figure S5). This metabolic pathway is transcriptionally regulated by complexes involving R2R3-MYB and basic helix-loop-helix (bHLH) transcription factors (Wang et al., 2020). The differential expression of *ADT, MYB* and *bHLH* transcripts in *A. pinsapo* roots and needles aligns with transcriptomic changes in response to climatic stress. In fact, bHLH122 has been functionally identified as a positive regulator of drought, NaCl, and osmotic stress responses in Arabidopsis (Liu et al., 2014). Recently, an HLH TF was reported to be a key regulatory factor of drought tolerance in poplar (Zhou et al., 2024). The lower content of flavonoids observed in YUN compared to RON (Fig. 7) supports the transcriptomic results, suggesting that flavonoid biosynthesis is negatively regulated in the stressed YUN forest. Downregulation of flavonoid biosynthesis in response to drought stress has been previously described in *Pinus taeda* and *Pinus halepensis* (Watkinson et al., 2003; Fox et al., 2018). However, the biological significance of this finding is not well understood because flavonoids have been described to play a protective role in the response of plants to abiotic stresses such as temperature and drought (Catalá et al., 2011; Nabakayashi et al., 2014).

Upregulation of tyrosine biosynthesis – a role of metabolites derived from tyrosine in the response of A. pinsapo to climatic stress

A noticeable finding of the present study is the upregulation of transcripts encoding enzymes involved in the decarboxylation of arogenate, catalyzed by a TyrA dehydrogenase enzyme, known as ADH, which plays a critical role in tyrosine biosynthesis (Fig. 4). Tyrosine is the precursor of a wide range of secondary metabolites that play essential roles in plant adaptation to environmental changes and to protect themselves against a range of biotic and abiotic stresses (Schenck and Maeda 2018). Among these compounds are antioxidants such as plastoquinone, tocopherols, betalains, and several alkaloids (Schenck and Maeda 2018). Interestingly, betalains, nitrogen-containing phenolic compounds structurally related to anthocyanins, are water-soluble and exhibiting a high capacity of protecting cells against deleterious effects of free radicals (Gandía-Herrero and Carmona 2016). Furthermore, alkaloids derived from tyrosine such as berberine, morphine, codeine and epinephrine, are also N-containing compounds. In the biosynthesis pathway for these secondary metabolites, tyrosine is first hydroxylated and subsequently converted to betalamic acid through the sequential action of cytochrome P450 and DOPA dyoxigenase (Polturak and Aharoni 2018). Transcripts encoding cytochrome P450, L-DOPA oxygenase, and amaranthin synthetase were highly abundant in the needles and roots of YUN trees at the end of the dry season (Table S6). The upregulation suggests a role of tyrosine-derived compounds in *A. pinsapo's* response to climatic stress.

Arogenate serves as a substrate for both ADT and ADH, with these two enzymes competing for a common intermediary metabolite. A shift in their transcriptional regulation suggests altered carbon flow from phenylalanine biosynthesis toward tyrosine biosynthesis (El-Azaz et al., 2023; 2024). Accordingly, our findings indicate that the downregulation of flavonoid biosynthesis in vulnerable trees coincides with the enhanced biosynthesis of tyrosine, likely providing antioxidant metabolites to mitigate stress during the dry season. An intriguing question arises from these findings: why is this metabolic shift more pronounced in the most stressed *A. pinsapo* populations? Likely, this could represent a good example of adaptive change that implies readjustments in the metabolism of phenolic antioxidants, as a mechanism of defense against the abiotic stresses such as increasing temperature and drought. This is consistent with the previously reported accumulation of tyrosine-derived metabolites in acclimation to high light and water stress ((Polturak and Aharoni, 2018)). In addition to their antioxidant ability, as it is the case of flavonoids, these phenolic compounds also represent a reservoir of nitrogen (N) and therefore may contribute to tree N economy under stressful conditions. It is well-known that arginine is a key amino acid for N storage in conifers under favorable conditions of growth (Llebrés et al., 2018; Cánovas et al., 2018); however, transcripts levels for key enzymes for arginine metabolism are downregulated in YUN needles (the location under more adverse climatic conditions) (Table S5). Taken together, the above findings suggest that stressed trees prioritize the biosynthesis of nitrogen-rich phenolics likely because they exhibit a dual function as antioxidants and as transient N storage. Metabolomic verification of secondary metabolites derived from aromatic amino acid pathways deserves further attention and should be a priority in future studies.

Differential modulation of the transcriptome in photosynthetic versus non-photosynthetic tissues

The total number of DEGs under stressed conditions (autumn) was significantly higher in needles compared to roots (Fig. 3). However, the

differences in gene expression levels observed in roots were higher than in needles suggesting that the effects of climate stress are firstly detected in roots (Fig. 4). These results agree with previous reports suggesting that roots are more sensitive to environmental stresses than aboveground tissues (de Miguel et al., 2016; Haas et al., 2021). Considering that the stress is primarily sensed in roots, the question arises: how is the signal transmitted to the aboveground tissues? In trees, abscisic acid has been proposed as a long-distance signal that communicates root stress to the aerial parts (Brunner et al., 2015). According to this, a decrease in the root cell turgor pressure caused by the water deficit may regulate stomatal closure in YUN trees' needles (Fig. 2).

Downregulation of WAT1 in the needles and the reduced assimilation rate observed in YUN trees may be consistent with stress signals received from roots at the end of the dry season. WAT1, a transmembrane protein required for secondary cell wall formation in fiber, is also known as UMAMIT 5 and functions as an auxin transporter involved in auxin homeostasis (Ranocha et al., 2013). Therefore, the high number of downregulated transcripts for WAT1 in the needles suggests the concomitant downregulation of tryptophan and indole metabolism. Interestingly, this downregulation of WAT1 was greater in needles, suggesting a major effect of stressful climatic conditions in the aerial part of the tree, where growth is taking place. These findings are in good agreement with the lower photosynthetic ability observed (Fig. 2). It has been described that inactivation of WAT1 mediates resistance to vascular bacterial and fungal pathogens in the vascular tissues of Arabidopsis (Denancé et al., 2013). Although the role of WAT1 has been associated with biotic stress in Arabidopsis, the results of the present study further suggest the implication of WAT1 in abiotic stress, likely triggering growth arrest and inhibition of cell elongation in photosynthetic tissues of *A. pinsapo* (Fig. 4).

In a previous study, an increased expression of transcripts for LEA proteins in *A. pinsapo* needles during the dry season was reported. This finding is confirmed here through the identification of hub genes belonging to the same family (Fig. 5). In roots, highly expressed genes encoding several LEA proteins (*ApLEA5, ApLEA24, ApLEA26, ApLEA30*) and dehydrins (*ApDHN4, ApDHN7, ApDHN16, ApDHN18, ApDHN26*) were identified. It was previously reported that ApLea30 is an ortholog of PaLea81, a water-stress related protein in the roots of *Picea Abies* (Haas et al. 2021). These data reinforce the potential role of *ApLea30* as a pivotal gene in the response of *A. pinsapo* and other conifers to climatic stresses. The localization of ApLEA30 in the plastid (Fig. 6) suggests a major role of this subcellular compartment in the response to stress. The chloroplast acts as a sensor in plant stress response, where numerous vital processes take place, such as the biosynthesis of aromatic amino acids, fatty acids, and secondary metabolites. It is also responsible for optimizing the production of metabolites, including the production of antioxidants, which serve as protective compounds against stress. Interestingly, the above-mentioned genes are integrated into a gene network alongside genes involved in the biosynthesis of tyrosine-derived compounds (*ADH2*) and those encoding regulatory genes (ERF061, YABBY5, NAC25). Notably, this network also includes *ApLEA30*, a gene whose evolutionary conservation across conifers was confirmed through a phylogenetic analysis of group D LEA proteins (Figure S6). This analysis revealed that ApLEA30 clusters closely with homologs from several *Abies* and *Pinus* species, highlighting its potential as a conserved feature associated with adaptation of conifer forest to Mediterranean basin conditions. Taken together, the data suggest that this gene network contains principal players involved in the sensing and resilience of *A. pinsapo* against climatic stress. Further research efforts are needed to functionally characterize the molecular and regulatory interactions occurring among members of this network. For example, the interaction of ApLEA30 and transcription factors within the network can be addressed through electrophoretic mobility shift assays and transactivation studies, as previously reported for other conifer genes (Craven-Bartle et al. 2013; Pascual et al. 2018; El-Azaz et al. 2020). This new knowledge will provide a better understanding of the molecular basis of forest resilience against the current threats of climate change.

In summary, molecular biology and functional genomics studies performed here provide new and useful knowledge for a better understanding of *A. pinsapo* forests' response to abiotic stresses and to unveil the molecular basis of mechanisms potentially implicated in their adaptive capacity. The identification of key genes involved in this response can be used as valuable molecular markers for studying the effects of increasing dryness and warming in the conifer forests of the Mediterranean basin.

Supporting information

Figure S1. Phylogenetic analysis of LEA sequences. *Pinus taeda* (Pta, blue diamonds), *Arabidopsis thaliana* (At, orange circles) and *Abies pinsapo* (Ap, green diamonds). The tree shows the distribution of sequences in nine families named from A to I. The analysis was performed after ClustalW type alignment and following the Maximum Parsimony method with 1000 bootstrap replicates using the program MEGA11 (Tamura et al., 2021).

Figure S2. Overview of the bioinformatic analysis pipeline.

Figure S3. Validation of transcriptome sequencing in (a) autumn and (b) spring samples (b). Experimental validation of RNAseq results for 12 DE transcripts through RT-qPCR (reverse transcription and quantitative polymerase chain reaction): ap_2991 (ApLEA30), ap_60,056 (UDP-glycosyltransferase), ap_65,968 (Arogenate dehydratase), ap_12,775 (WAT1-related protein), ap_28,951 (NAC transcription factor), ap_71,257 (Phospho-2-dehydro-3-deoxyheptonate aldolase), ap_556 (Alpha-trehalose-phosphate synthase), ap_4904 (Chalcone synthase), ap_96 (Flavanone-3-hydroxylase), ap_20,750 (Shikimate dehydrogenase), ap_4147 (PfkB domain-containing protein), ap_15,225 (Protein NRT1 family). Bars correspond to transcript abundance quantified by RT−qPCR in needles (green) and roots (grey), while red dots corresponds to RNA-seq analyses.

Figure S4. Biological processes significantly enriched in the GO analysis, needles (a), roots (b).

Figure S5. Phylogenetic analysis of ADT sequences. Phylogenetic tree showing the distribution of ADTs from *Pinus pinaster* (Pp), *Arabidopsis thaliana* (At) and the ADT transcripts found in *Abies pinsapo* (ap). Transcripts from *Abies pinsapo* corresponding to type I (green) and II (yellow) ADTs (El-Azaz *et al*. 2022) are highlighted in bold. The analysis was performed after Muscle type alignment and following the Maximum Likehood method with 1000 bootstrap replicates using the program MEGA 11 (https://doi.org/10.1093/molbev/msab120).

Figure S6. Phylogenetic tree of group D of LEA proteins in conifers. The analysis was performed after ClustalW type alignment and following the Maximum Parsimony method with 1000 bootstrap replicates using the program MEGA 11 (https://doi.org/10.1093/molbev/msab120). Diamonds in different colours indicate different species: purple (*Picea glauca*), lilac (*Picea abies*), green (Ap: *Abies pinsapo*), light green (*Abies alba*), emerald green (*Abies balsamea*), blue (Pta: *Pinus taeda*), dark blue (*Pinus pinaster*), black (*Pinus nigra*), yellow (*Pinus halepensis*), brown (*Taxus baccata*) and pink (*Cryptomeria japonica*). Proteins with high similarity to ApLEA30 are indicated in bold.

Table S1. List of primers used in this work.

Table S2. Protein sequences used for phylogenetic analysis

Table S3. Summary of sequencing metrics.

Table S4. Mapping metrics.

Table S5. GO terms based on transcriptome annotations.

Table S6 List of genes differentially regulated in needles and roots in spring and autumn.

Table S7. Upregulated transcripts in the needles and roots of YUN trees at the end of the dry season.

CRediT authorship contribution statement

Irene Blanca-Reyes: Validation, Methodology, Investigation. **María**

Torés-España: Validation, Software, Methodology, Data curation. **Victor Lechuga:** Writing – review & editing, Resources, Methodology, Investigation. **María Teresa Llebrés:** Writing – review & editing, Visualization, Validation, Methodology, Formal analysis. **Fernando N. de la Torre:** Writing – review & editing, Validation, Resources, Formal analysis, Data curation. **José A. Carreira:** Writing – review & editing, Validation, Supervision, Formal analysis, Data curation, Conceptualization. **Concepción Avila:** Writing – review & editing, Visualization, Validation, Supervision, Funding acquisition, Formal analysis, Data curation, Conceptualization. **Francisco M. Cánovas:** Writing – original draft, Visualization, Validation, Supervision, Investigation, Funding acquisition, Formal analysis, Data curation, Conceptualization. **Vanessa Castro-Rodríguez:** Writing – original draft, Visualization, Validation, Supervision, Resources, Methodology, Investigation, Formal analysis, Data curation.

Declaration of competing interest

The authors declare that they have no known competing financial interests or personal relationships that could have appeared to influence the work reported in this paper.

Acknowledgements

We would like to thank José López-Quintanilla and Rafael Haro-Ramos for providing access to the forests of the National Park "Sierra de las Nieves", collaborating in the sampling of plant material and their valuable advice. This research was supported by grants from the Spanish "Agencia Estatal de Investigación (AEI), Ministerio de Ciencia, Innovación y Universidades", (TED2021-129691B-I00 and PID2021-125040OB-I00). IBR was supported by a predoctoral contract for the training of doctors (FPI) from AEI.

The authors thankfully acknowledge the computer resources (Picasso Supercomputer), and technical assistance provided by the SCBI (Supercomputing and Bioinformatics) center of the University of Malaga.

Supplementary materials

Supplementary material associated with this article can be found, in the online version, at doi:10.1016/j.stress.2025.101009.

Data availability

Data will be made available on request.

References

Aitken, S.N., Yeaman, S., Holliday, J.A., Wang, T.L., Curtis-McLane, S., 2008. Adaptation, migration or extirpation: climate change outcomes for tree populations. Evol. Appl. 1, 95–111.

Allen, C.D., K Macalady, A.K., Haroun Chenchouni, H., Dominique Bachelet, D., et al., 2010. A global overview of drought and heat-induced tree mortality reveals emerging climate change risks for forests. For. Ecol. Manag. 259, 660–684. https://doi.org/10.1016/j.foreco.2009.09.001.

Allona, I., Kirst, M., Boerjan, W., Strauss, S., Sederoff, R., 2019. Forest genomics and biotechnology. Front. Plant Sci. 10, 1187.

Alexa, A., Rahnenfuhrer, J., 2024. TopGO: enrichment analysis for gene ontology. R Package Version 2.56.0.

Anderegg, W.R.L., Anderegg, L.D.L., Kerr, K.L., Trugman, A.T., 2019. Widespread drought-induced tree mortality at dry range edges indicates that climate stress exceeds species' compensating mechanisms. Glob. Change Biol. 25, 3793–3802. https://doi.org/10.1111/gcb.14771.

Blanca-Reyes, I., Lechuga, V., Llebrés, M.T., Carreira, J.A., Ávila, C., Cánovas, F.M., Castro-Rodríguez, V., 2024. Under stress: searching for genes involved in the response of *Abies pinsapo* Boiss. To climate change. Int. J. Mol. Sci. 25, 4820.

Blanco-Cano, L., Navarro-Cerrillo, R.M., González-Moreno, P., 2022. Biotic and abiotic effects determining the resilience of conifer mountain forests: the case study of the endangered Spanish fir. For. Ecol. Manag. 520, 120356.

Brockerhoff, E.G., Barbaro, L., Castagneyrol, B., Forrester, D.I., et al., 2017. Forest biodiversity, ecosystem functioning and the provision of ecosystem services. Biodivers. Conserv. 26, 3005–3035.

Brunner, I., Herzog, C., Dawes, M.A., Arend, M., Sperisen, C., 2015. How tree roots respond to drought. Front. Plant Sci. 6, 152207.

Buchfink, B., Reuter, K., Drost, H., 2021. Sensitive protein alignments at tree-of-life scale using DIAMOND. Nat. Methods 18, 366–368. https://doi.org/10.1038/s41592-021-01101-x.

Bustin, S.A., Benes, V., Garson, J.A., Hellemans, J., Huggett, J., Kubista, M., Mueller, R., Nolan, T., Pfaffl, M.W., Shipley, G.L., et al., 2009. The MIQE Guidelines: minimum information for publication of quantitative real-time PCR experiments. Clin. Chem. 55, 611–622.

Canales, J., Rueda-López, M., Craven-Bartle, B., Avila, C., Cánovas, F., 2012. Novel insights into regulation of asparagine synthetase in Conifers. Front. Plant Sci. 3, 100.

Cañas, R.A., Canales, J., Gómez-Maldonado, J., Ávila, C., Cánovas, F.M., 2014. Transcriptome analysis in maritime pine using laser capture microdissection and 454 pyrosequencing. Tree Physiol. 34, 1278–1288.

Cañas, R.A., Pascual, M.B., de la Torre, F.N., Ávila, C., Cánovas, F.M., 2019. Resources for conifer functional genomics at the omics era. In: Cánovas, F.M. (Ed.), Molecular Physiology and Biotechnology of Trees. Academic Press, MA, USA, pp. 39–76.

Cánovas, F.M., Cañas, R.A., de la Torre, F.N., Pascual, M.B., Castro-Rodríguez, V., Avila, C., 2018. Nitrogen metabolism and biomass production in forest trees. Front. Plant Sci. 9, 1449. https://doi.org/10.3389/fpls.2018.01449.

Castro-Rodríguez, V. 2024. PacBio sequencing for Spanish fir resilience: genomic insights for sustainable forest management, IUFRO Tree Biotech 2024, Annapolis, USA. https://treebiotech.org/.

Catalá, R., Medina, J., Salinas, J., 2011. Integration of low temperature and light signaling during cold acclimation response in Arabidopsis. Proc. Natl. Acad. Sci. USA 108 (39). https://doi.org/10.1073/pnas.1107161108.

Cobo-Simón, I., Maloof, J.N., Li, R., Amini, H., Méndez-Cea, B., García-García, I., Gómez-Garrido, J., Esteve-Codina, A., Dabad, M., Alioto, T., Wegrzyn, J.L., Seco, J.I., Linares, J.C., Gallego, F.J., 2023. Contrasting transcriptomic patterns reveal a genomic basis for drought resilience in the relict fir *Abies pinsapo* Boiss. Tree Physiol. 43, 314–334. https://doi.org/10.1093/treephys/tpac115.

Corea, O.R.A., Bedgar, D.L., Davin, L.B., Lewis, N.G., 2012a. The arogenate dehydratase gene family: towards understanding differential regulation of carbon flux through phenylalanine into primary versus secondary metabolic pathways. Phytochemistry 82, 22–37.

Corea, O.R.A., Ki, C., Cardenas, C.L., Kim, S.J., Brewer, S.E., Patten, A.M., Davin, L.B., Lewis, N.G., 2012b. Arogenate dehydratase isoenzymes profoundly and differentially modulate carbon flux into lignins. J. Biol. Chem. 287, 11446–11459.

Craven-Bartle, B., Pascual, M.B., Cánovas, F.M., Avila, C., 2013. A Myb transcription factor regulates genes of the phenylalanine pathway in maritime pine. Plant J. 74, 755–766.

Denancé, N., Ranocha, P., Oria, N., Barlet, X., et al., 2013. Arabidopsis wat1 (walls are thin1)-mediated resistance to the bacterial vascular pathogen, *Ralstonia solanacearum*, is accompanied by cross-regulation of salicylic acid and tryptophan metabolism. Plant J. 73, 225–239.

De La Torre, A.R., Birol, I., Bousquet, J., Ingvarsson, P.K., Jansson, S., Jones, S.J., Keeling, C.I., MacKay, J., Nilsson, O., Ritland, K., Street, N., Yanchuk, A., Zerbe, P., Bohlmann, J., 2014. Insights into conifer giga-genomes. Plant Physiol. 166, 1724–1732. https://doi.org/10.1104/pp.114.248708.

De La Torre, A.R., Sekhwal, M.K., Puiu, D., Salzberg, S.L., Scott, A.D., Allen, B., Neale, D. B., Chin, A.R.O., Buckley, T.N., 2022. Genome-wide association identifies candidate genes for drought tolerance in coast redwood and giant sequoia. Plant J. 109, 7–22. https://doi.org/10.1111/tpj.15592.

DeSoto, L., Cailleret, M., Sterck, F., Jansen, S., et al., 2020. Low growth resilience to drought is related to future mortality risk in trees. Nat. Commun. 11, 545. https://doi.org/10.1038/s41467-020-14300-5.

de María, N., Guevara, M.Á., Perdiguero, P., Vélez, M.D., Cabezas, J.A., López-Hinojosa, M., Li, Z., Díaz, L.M., Pizarro, A., Mancha, J.A., et al., 2020. Molecular study of drought response in the Mediterranean conifer *Pinus pinaster* Ait.: differential transcriptomic profiling reveals constitutive water deficit-independent drought tolerance mechanisms. Ecol Evol. 10, 9788–9807.

de Miguel, M., Guevara, M.Á., Sánchez-Gómez, D., de María, N., Díaz, L.M., Mancha, J. A., Fernández de Simón, B., Cadahía, E., Desai, N., Aranda, I., et al., 2016. Organ-specific metabolic responses to drought in *Pinus pinaster* Ait. Plant Physiol. Biochem. 102, 17–26.

De Silva, K.K., Dunwell, J.M., Wickramasuriya, A.M., 2022. Weighted gene correlation network analysis (WGCNA) of Arabidopsis somatic embryogenesis (SE) and identification of key gene modules to uncover SE-associated HuB genes. Int. J. Genomics 1–24. https://doi.org/10.1155/2022/7471063.

El-Azaz, J., de la Torre, F., Ávila, C., Cánovas, F.M., 2016. Identification of a small protein domain present in all plant lineages that confers high prephenate dehydratase activity. Plant J. 87, 215–229.

El-Azaz, J., de La Torre, F., Pascual, M.B., Debille, S., Canlet, F., Harvengt, L., Trontin, J. F., Ávila, C., Cánovas, F.M., 2020. Transcriptional analysis of arogenate dehydratase genes identifies a link between phenylalanine biosynthesis and lignin biosynthesis. J. Exp. Bot. 71, 3080–3093.

El-Azaz, J., Cánovas, F.M., Barcelona, B., Ávila, C., de la Torre, F., 2022. Deregulation of phenylalanine biosynthesis evolved with the emergence of vascular plants. Plant Physiol. 188, 134–150.

El-Azaz, J., Moore, B., Takeda-Kimura, Y., Yokoyama, R., Wijesingha Ahchige, M., Chen, X., Schneider, M., Maeda, H.A., 2023. Coordinated regulation of the entry and exit steps of aromatic amino acid biosynthesis supports the dual lignin pathway in grasses. Nat. Commun. 14, 7242. https://doi.org/10.1038/s41467-023-42587-7.

El-Azaz, J., Maeda, H.A., 2024. A simplified liquid chromatography-mass spectrometry methodology to probe the shikimate and aromatic amino acid biosynthetic pathways in plants. Plant J. 120, 2286–2304. https://doi.org/10.1111/tpj.17105. Epub ahead of print. PMID: 39466904.

Felipe-Lucia, M.R., Soliveres, S., Penone, C., et al., 2018. Multiple forest attributes underpin the supply of multiple ecosystem services. Nat. Commun. 9, 4839.

Fox, H., Doron-Faigenboim, A., Kelly, G., Bourstein, R., Attia, Z., Zhou, J., Moshe, Y., Moshelion, M., David-Schwartz, R., 2018. Transcriptome analysis of *Pinus halepensis* under drought stress and during recovery. Tree Physiol. 38, 423–441.

Gandía-Herrero, F., Escribano, J., García-Carmona, F., 2016. Biological activities of plant pigments betalains. Crit. Rev. Food Sci. Nutr. 56 (6). https://doi.org/10.1080/10408398.2012.740103.

Gao, J., Lan, T., 2016. Functional characterization of the late embryogenesis abundant (LEA) protein gene family from *Pinus tabuliformis* (Pinaceae) in *Escherichia coli*. Sci. Rep. 6, 19467. https://doi.org/10.1038/srep19467.

Garabagi, F., Gilbert, E., Loos, A., McLean, M.D., Hall, J.C., 2012. Utility of the P19 suppressor of gene-silencing protein for production of therapeutic antibodies in Nicotiana expression hosts. Plant Biotechnol. J. 10, 1118–1128. https://doi.org/10.1111/j.1467-7652.2012.00742.x.

Gazol, A., Camarero, J.J., Vicente-Serrano, S.M., Sánchez-Salguero, R., Gutiérrez, E., de Luis, M., Sangüesa-Barreda, G., Novak, K., Rozas, V., Tíscar, P.A., Linares, J.C., Martín-Hernández, N., Martínez del Castillo, E., Ribas, M., García-González, I., Silla, F., Camisón, A., Génova, M., Olano, J.M., Longares, L.A., Hevia, A., Tomás-Burguera, M., Galván, J.D, 2018. Forest resilience to drought varies across biomes. Glob. Change Biol. 24, 2143–2158.

Haas, J.C., Vergara, A., Serrano, A.R., Mishra, S., Hurry, V., Street, N.R., 2021. Candidate regulators and target genes of drought stress in needles and roots of Norway spruce. Tree Physiol. 41, 1230–1246.

Hammer, Ø., Harper, D.A.T., Ryan, P.D., 2001. Past: paleontological statistical software package for education and data analysis. Palaeontol Electronica 4, 9.

Hartmann, H., Bastos, A., Das, A.J., Esquivel-Muelbert, A., et al., 2022. Climate change risks to global forest health: emergence of unexpected events of elevated tree mortality worldwide. Annu. Rev. Plant Biol. 73, 673–702.

He, X., Anderson, J.C., Pozo, O.d., Gu, Y.-Q., Tang, X., Martin, G.B., 2004. Silencing of subfamily I of protein phosphatase 2A catalytic subunits results in activation of plant defense responses and localized cell death. Plant J. 38, 563–577. https://doi.org/10.1111/j.1365-313X.2004.02073.x.

Hincha, D.K., Thalhammer, A., 2012. LEA proteins: iDPs with versatile functions in cellular dehydration tolerance. Biochem. Soc. Trans. 40, 1000–1003. https://doi.org/10.1042/BST20120109.

Huerta-Cepas, J., Szklarczyk, D., Heller, D., Hernández-Plaza, A., Forslund, S.K., Cook, H., Mende, D.R., Letunic, I., Rattei, T., Jensen, L.J., Von Mering, C., Bork, P., 2018. eggNOG 5.0: a hierarchical, functionally and phylogenetically annotated orthology resource based on 5090 organisms and 2502 viruses. Nucleic Acids Res. 47, D309–D314. https://doi.org/10.1093/nar/gky1085.

Langfelder, P., Horvath, S., 2008. WGCNA: an R package for weighted correlation network analysis. BMC Bioinformatics 9. https://doi.org/10.1186/1471-2105-9-559.

Lawson, T., Vialet-Chabrand, S., 2019. Speedy stomata, photosynthesis and plant water use efficiency. New Phytol. 221, 93–98.

Lechuga, V., Carraro, V., Viñegla, B., Carreira, J.A., Linares, J.C., 2017. Managing drought-sensitive forests under global change. Low competition enhances long-term growth and water uptake in *Abies pinsapo*. For. Ecol. Manag. 406, 72–82. https://doi.org/10.1016/j.foreco.2017.10.017.

Lechuga, V., Carraro, V., Viñegla, B., Carreira, J.A., Linares, J.C., 2019. Carbon limitation and drought sensitivity at contrasting elevation and competition of *Abies pinsapo* forests. Does experimental thinning enhance water supply and carbohydrates? Forests 10, 1132. https://doi.org/10.3390/f10121132.

Li, W., Wang, L., Wu, Y., Yuan, Z., Zhou, J., 2020. Weighted gene co-expression network analysis to identify key modules and hub genes associated with atrial fibrillation. Int. J. Mol. Med. 45, 401–416. https://doi.org/10.3892/ijmm.2019.4416.

Linares, J.C., Camarero, J.J., Carreira, J.A., 2009. Interacting effects of changes in climate and forest cover on mortality and growth of the southernmost European fir forests. Glob. Ecol. Biogeogr. 18, 485–497. https://doi.org/10.1111/j.1466-8238.2009.00465.x.

Linares, J.C., 2011. Biogeography and evolution of *Abies* (Pinaceae) in the Mediterranean Basin: the roles of long-term climatic change and glacial refugia. J. Biogeogr. 43, 1–12. https://doi.org/10.1111/j.1365-2699.2010.02458.x.

Linares, J.C., Camarero, J.J., Carreira, J.A., 2010. Competition modulates the adaptation capacity of forests to climatic stress: insights from recent growth decline and death in relict stands of the Mediterranean fir *Abies pinsapo*. J. Ecol. 98, 592–603. https://doi.org/10.1111/j.1365-2745.2010.01645.x.

Linares, J.C., Covelo, F., Carreira, J.A., Merino, J.A., 2012. Phenological and water-use patterns underlying maximum growing season length at the highest elevations: implications under climate change. Tree Physiol. 32, 161–170.

Liu, W., Tai, H., Li, S., Gao, W., Zhao, M., Xie, C., Li, W.X., 2014. bHLH122 is important for drought and osmotic stress resistance in Arabidopsis and in the repression of ABA catabolism. New Phytol. 201, 1192–1204. https://doi.org/10.1111/nph.12607.

Llebrés, M.T., Pascual, M.B., Debille, S., Trontin, J.F., Harvengt, L., Avila, C., Cánovas, F. M., 2018. The role of arginine metabolic pathway during embryogenesis and germination in maritime pine (*Pinus pinaster* Ait.). Tree Physiol. 38, 471–484. https://doi.org/10.1093/treephys/tpx133.

Love, M.I., Huber, W., Anders, S., 2014. Moderated estimation of fold change and dispersion for RNA-seq data with DESeq2. Genome Biol. 15, 550. https://doi.org/10.1186/s13059-014-0550-8.

Manjarrez, L.F., Guevara, M.Á., de María, N., Vélez, M.D., Cobo-Simón, I., López-Hinojosa, M., Cabezas, J.A., Mancha, J.A., Pizarro, A., Díaz-Sala, M.C., Cervera, M. T., 2024a. Maritime pine rootstock genotype modulates gene expression associated with stress tolerance in grafted stems. Plants 13, 1644.

Manjarrez, L.F., de María, N., Vélez, M.D., Cabezas, J.A., Mancha, J.A., Ramos, P., Pizarro, A., Blanco-Urdillo, E., López-Hinojosa, M., Cobo-Simón, I., Guevara, M.Á., Díaz-Sala, M.C., Cervera, M.T., 2024b. Comparative stem transcriptome analysis reveals pathways associated with drought tolerance in maritime pine grafts. Int. J. Mol. Sci. 25, 9926. https://doi.org/10.3390/ijms25189926.

Mina, M., Bugmann, H., Cordonnier, T., Irauschek, F., Klopcic, M., Pardos, M., Cailleret, M., 2017. Future ecosystem services from European mountain forests under climate change. J. Appl. Ecol. 54, 389–401. https://doi.org/10.1111/1365-2664.12772.

Moriya, Y., Itoh, M., Okuda, S., Yoshizawa, A.C., Kanehisa, M., 2007. KAAS: an automatic genome annotation and pathway reconstruction server. Nucleic Acids Res. 35, W182–W185. https://doi.org/10.1093/nar/gkm321.

Nakabayashi, R., Mori, T., Saito, K., 2014. Alternation of flavonoid accumulation under drought stress in *Arabidopsis thaliana*. Plant Signal Behav. 9, e29518. https://doi.org/10.4161/psb.29518. PMID: 25763629; PMCID: PMC4203635.

Navarro-Cerrillo, R.M., González-Moreno, P., Ruiz-Gómez, F.J., Sánchez-Cuesta, R., Gazol, A., Camarero, J.J., 2022. Drought stress and pests increase defoliation and mortality rates in vulnerable *Abies pinsapo* forests. For. Ecol. Manag. 504, 119824. https://doi.org/10.1016/j.foreco.2021.119824.

Ortigosa, F., Ávila, C., Rubio, L., Álvarez-Garrido, L., Carreira, J.A., Cañas, R.A., Cánovas, F.M., 2022. Transcriptome analysis and intraspecific variation in spanish fir (*Abies pinsapo* Boiss.). Int. J. Mol. Sci. 23, 9351. https://doi.org/10.3390/ijms23169351. PMID: 36012612; PMCID: PMC9409315.

Pascual, M.B., El-Azaz, J., de la Torre, F.N., Cañas, R.A., Avila, C., Cánovas, F.M., 2016. Biosynthesis and metabolic fate of phenylalanine in conifers. Front. Plant Sci. 7, 1030.

Pascual, M.B., Llebrés, M.T., Craven-Bartle, B., Cañas, R.A., Cánovas, F.M., Ávila, C., 2018. *PpNAC1*, a main regulator of phenylalanine biosynthesis and utilization in maritime pine. Plant Biotechnol. J. 16, 1094–1104.

Pérez-González, A., Marconi, M., Cobo-Simón, I., Méndez-Cea, B., Perdiguero, P., Linacero, R., Linares, J.C., Gallego, F.J., 2018. *Abies pinsapo* Boiss. Transcriptome sequencing and molecular marker detection: a novel genetic resources for a relict Mediterranean fir. For. Sci. 64, 6.

Polturak, G., Aharoni, A., 2018. La Vie en Rose": biosynthesis, sources, and applications of betalain pigments. Mol. Plant 11, 7–22.

Ranocha, P., Denancé, N., Vanholme, R., Freydier, A., Martinez, Y., Hoffmann, L., Köhler, L., Pouzet, C., Renou, J-P., Sundberg, B., Boerjan, W., Goffner, D., 2010. *Walls are thin 1* (*WAT1*), an *Arabidopsis* homolog of *Medicago truncatula NODULIN21*, is a tonoplast-localized protein required for secondary wall formation in fibers. Plant J. 63, 469–483.

Ranocha, P., Dima, O., Nagy, R., Felten, J., Corratge-Faillie, C., Novak, O., Morreel, K., Lacombe, B., Martinez, Y., Pfrunder, S., Jin, X., Renou, J.P., Thibaud, J.B., Ljung, K., Fischer, U., Martinoia, E., Boerjan, W., Goffner, D., 2013. Arabidopsis WAT1 is a vacuolar auxin transport facilitator required for auxin homoeostasis. Nat. Commun. 4, 3625. https://doi.org/10.1038/ncomms3625.

Ritz, C., Spiess, A.-N., 2008. qpcR: an R package for sigmoidal model selection in quantitative real-time polymerase chain reaction analysis. Bioinformatics 24, 1549–1551.

Rokitta, S.D., Von Dassow, P., Rost, B., John, U., 2005. Blast2GO: a universal tool for annotation, visualization and analysis in functional genomics research. Bioinformatics 21, 3674–3676. https://doi.org/10.1093/bioinformatics/bti610.

Rossi, G., Woods, F.M., Leisner, C.P., 2022. Quantification of total phenolic, anthocyanin, and flavonoid content in a diverse panel of blueberry cultivars and ecotypes. HortSci 57 (8), 901–909. https://doi.org/10.21273/HORTSCI16647-22.

Sánchez-Salguero, R., Ortíz, C., Covelo, F., Ochoa, V., García-Ruíz, R., Seco, J.I., Carreira, J.A., Merino, J.A., Linares, J.C., 2015. Regulation of water use in the southernmost European fir (*Abies pinsapo* Boiss.): drought avoidance matters. Forests 6, 2241–2260. https://doi.org/10.3390/f6062241.

Sánchez-Salguero, R., Camarero, J.J., Carrer, M., Gutiérrez, E., Alla, A.Q., Andreu-Hayles, L., Hevia, A., Koutavas, A., Martínez-Sancho, E., Nola, P., Papadopoulos, A., Pasho, E., Toromani, E., Carreira, J.A., Linares, J.C., 2017. Climate extremes and predicted warming threaten Mediterranean Holocene firs forests refugia. Proc. Natl. Acad. Sci. USA 114, E10142–E10150.

Saelens, W., Cannoodt, R., Saeys, Y., 2018. A comprehensive evaluation of module detection methods for gene expression data. Nat. Commun. 9 (1). https://doi.org/10.1038/s41467-018-03424-4.

Sayers, E.W., Bolton, E.E., Brister, J.R., Canese, K., Chan, J., Comeau, D.C., Connor, R., Funk, K., Kelly, C., Kim, S., Madej, T., Marchler-Bauer, A., Lanczycki, C., Lathrop, S., Lu, Z., Thibaud-Nissen, F., Murphy, T., Phan, L., Skripchenko, Y., Tse, T., Wang, J., Williams, R., Trawick, B.W., Pruitt, K.D., Sherry, S.T., 2021. Database resources of the national center for biotechnology information. Nucleic Acids Res. 50 (D1), D20–D26. https://doi.org/10.1093/nar/gkab1112.

Schenck, C.A., Maeda, H.A., 2018. Tyrosine biosynthesis, metabolism, and catabolism in plants. Phytochemistry 149, 82–102.

Sena, J.S., Giguère, I., Rigault, P., Bousquet, J., Mackay, J., 2018. Expansion of the dehydrin gene family in the Pinaceae is associated with considerable structural diversity and drought-responsive expression. Tree Physiol. 38, 442–456. https://doi.org/10.1093/treephys/tpx125.

Shannon, P., Markiel, A., Ozier, O., Baliga, N.S., Wang, J.T., Ramage, D., Amin, N., Schwikowski, B., Ideker, T., 2003. Cytoscape: a software environment for integrated models of biomolecular interaction networks. Genome Res. 13, 2498–2504. https://doi.org/10.1101/gr.1239303.

Street, N., 2019. Genomics of forest trees. In: Cánovas, F.M. (Ed.), Molecular Physiology and Biotechnology of Trees. Academic Press, Cambridge, MA, USA, pp. 1–37.
Tamura, K., Stecher, G., Kumar, S., 2021. MEGA11: molecular evolutionary genetics analysis version 11. Mol. Biol. Evol. 38, 3022–3027. https://doi.org/10.1093/molbev/msab120.
Wang, X.C., Wu, J., Guan, M.L., Zhao, C.H., Geng, P., Zhao, Q., 2020. Arabidopsis MYB4 plays dual roles in flavonoid biosynthesis. Plant J. 101, 637–652.
Watkinson, J.I., Sioson, A.A., Vasquez-Robinet, C., Shukla, M., Kumar, D., Ellis, M., Heath, L.S., Ramakrishnan, N., Chevone, B., Watson, L.T., van Zyl, L., Egertsdotter, U., Sederoff, R.R., Grene, R., 2003. Photosynthetic acclimation is reflected in specific patterns of gene expression in drought-stressed loblolly pine. Plant Physiol. 133, 1702–1716. https://doi.org/10.1104/pp.103.026914.
Yu, G., Wang, L., Han, Y., He, Q., 2012. clusterProfiler: an R package for comparing biological themes among gene clusters. Omics 16, 284–287. https://doi.org/10.1089/omi.2011.0118.
Zhou, M., Su, R.N., Charyberdiyev, E., Peng, N.F., Li, X., Chi, Y., Li, Y., Gao, C., Wang, C., 2024. PdbbHLH1 transcription factor improved drought tolerance of *Populus davidiana* × *P. bolleana*. Ind. Crop. Prod. 222, 119–683.